Multiple Shock Impulse Response Functions

Terri van der Zwan*

October 2023

Abstract

This paper introduces multiple shock impulse response functions, which consider the cumulative effects of simultaneous shocks within one period. The concept generalizes individual shock impulse response functions, accounts for the dependence between shocks, and is applicable to various multivariate time series models. It is relevant for identifying underlying primitive structural shocks and using regional shocks as global structural proxies. Simulation studies highlight its necessity for accurately interpreting the total effect of shocks and mitigating potential temporal aggregation issues. Applied to a global vector autoregression framework for France, Germany, Italy, and Spain, multiple shock impulse response functions offer insights into monetary policy dynamics during uncertainty spikes and serve as a stress test. For area-wide equity shocks, they align more closely with long-term theoretical expectations than the traditional GDP-weighted method, highlighting their ability in capturing economic dynamics.

Keywords: *Impulse response analysis, generalized impulse response functions, simultaneous shocks, multivariate time series models, temporal aggregation*

JEL classification codes: *C32, C53, E44, E52, G10*

*Erasmus School of Economics, Erasmus University Rotterdam; Tinbergen Institute. Corresponding email: t.vanderzwan@ese.eur.nl. I would like to thank Carlos Avenancio-León, Annika Camehl, Eva Janssens, Erik Kole, Andreas Pick, Bernd Schwaab, Michel van der Wel, for valuable discussions and comments, as well as the participants of the 12th ECB Conference on Forecasting Techniques for their input. I am grateful for the *Fulbright Promovendus Grant* and the *Erasmus Trustfonds' STOER fonds* for funding my research visit to University of California San Diego, and to Allan Timmermann for hosting. All errors are my own. The latest version is available here.

1 Introduction

Impulse response function (IRF) analysis is a widely employed tool to examine the dynamic responses of multivariate systems to unexpected shocks or disturbances, and is useful to provide insights into the transmission mechanisms and feedback effects within the system.[1]

Impulse response analysis (Sims, 1980; Koop et al., 1996; Pesaran and Shin, 1998) typically requires identifying assumptions on relations between variables in the system, which are often too restrictive. While most empirical applications primarily focus on the effect of individual shocks, in times of crisis, economic and financial variables seem to be increasingly connected (Billio et al., 2012; Hubrich and Tetlow, 2015), which makes it more likely that multiple shocks occur within a short period of time. This might pose a problem where the measurement frequency of the data is insufficient. Data at a lower frequency can obscure causal information because multiple shocks happening at a higher frequency may be aggregated within one period of the lower frequency data (i.e., temporal aggregation problem). Therefore, it is crucial to account for these simultaneous shocks that we observe within one period of the measurement frequency.

This paper introduces multiple shock impulse response functions. This method enables investigation of the total effect of simultaneous model shocks taking place within the same period of time. It takes into account the dependence between the model shocks, and allows us to examine the cumulative and interactive impacts of multiple simultaneous shocks on a system. This concept is general, as it pertains to a wide variety of multivariate time series models, and it is a generalization of the individual shock generalized impulse response functions. This tool is particularly useful in scenarios where, for instance,the combined effect of the model shocks captures an underlying primitive shock (Ramey, 2016). Next to that, it facilitates the use of region-specific model shocks collectively acting as proxies for a single underlying global structural shock.

To illustrate the properties and applicability of multiple shock impulse response functions, we consider a first order vector autoregression. We derive the closed form solutions of

[1]Impulse response analysis was popularized by Sims (1972, 1980), who linked the dynamic stochastic general equilibrium models to vector autoregression models and their shocks. See Fernández-Villaverde et al. (2007) for details on the mapping of these structural macroeconomic models to the VAR specification.

the orthogonalized, generalized and multiple shock IRFs, and discuss their relation to each other. Using a set of data generating processes, we show that the multiple shock impulse response functions are necessary to accurately analyze the total effect of model shocks occurring simultaneously. Summing the individual impulse responses alone can lead to substantial over- or underestimation, as the extent of this discrepancy relies on the correlation between the model shocks. In a mixed-frequency setting based on Ghysels (2016), we demonstrate the usefulness of multiple shock impulse response functions in addressing potential temporal aggregation issues in case of multiple shocks occurring within the same lower frequency period. The multiple shock impulse response functions provide a more accurate approximation to the true high-frequency structural shocks compared to the summed low-frequency individual orthogonalized and generalized impulse responses. This demonstrates the efficacy of multiple shock impulse response analysis at a lower frequency in capturing the combined effects of multiple structural shocks occurring at higher frequencies.

We show the practical relevance of our multiple shock impulse response functions in context of a global vector autoregression framework (Pesaran et al., 2004) focusing on four economies; France, Germany, Italy and Spain. This framework allows for modeling direct effects of Euro area, and country-specific shocks and for cross-country interactions. Our primary focus is on the effect of a monetary policy shock and uncertainty shocks occurring in lower credit rating countries in the Euro area simultaneously within a one month time frame, as well as the collective impact of negative equity shocks across all countries. A monetary policy shock can induce a shock in financial uncertainty, altering the perception of systematic risk. During the European debt crisis, the European Central Bank's (ECB) decision to raise interest rates amplified financial uncertainty in vulnerable EMU countries. These changes typically occur within a month, underscoring the need for a framework that can analyze the impact of multiple shocks happening within one period. Additionally, we consider an area-wide negative equity shock. As the model lacks a dominant economy, it is not suitable to use a single variable as a proxy for an area-wide shock. We therefore focus on all country-specific equity indices to represent the aggregate Euro area equity index.

Using multiple shock impulse response functions is particularly beneficial in this context, as it helps to overcome temporal aggregation issues and it does not require assumptions on

the ordering of variables. The latter can be problematic as the contemporaneous relation between monetary policy and uncertainty remains ambiguous (see, e.g., Jurado et al., 2015), and the ordering of countries in the framework is unclear (Dees et al., 2007). We use the measure of Jarociński and Karadi (2020) as a proxy for a monetary policy shock, and the model residuals of Italy and Spain's country-specific stress indices as a proxy for uncertainty. We identify the equity shock using the model residuals of the country-specific stock indices. Our sample runs from January 1999 until October 2022. The model parameters are estimated using a Bayesian estimation procedure.

For the orthogonalized, generalized and multiple shock IRF concepts, we find responses consistent with economic theory. The interaction between a monetary policy shock and uncertainty shocks in Italy and Spain significantly amplify the effects compared to a monetary policy shock alone. This is especially pronounced in the adverse impact on real GDP, which we observe to be roughly double in magnitude. It is crucial to recognize that uncertainty shocks originating from Southern European countries can also influence France and Germany. Utilizing the multiple shock impulse response functions in this scenario provides valuable insights into the dynamics of monetary policy during spikes of uncertainty. It can serve as a stress test, gauging the resilience and potential reactions of economies to additional uncertainty. Clear and direct communication from the ECB could potentially mitigate these uncertainties. In our analysis of an area-wide negative equity shock, the multiple shock approach produces responses that align more closely with theoretical expectations, with effects naturally diminishing over time. This is distinct from the GDP-weighted average of country-specific equity shocks, a method often adopted in existing literature. While both methodologies produce comparable outcomes in the short-term, the responses from the latter tend to diverge as time progresses. This demonstrates the advantage of the multiple shock approach in capturing more consistent and theoretically aligned long-term dynamics.

The remainder of this paper is structured as follows. In Section 2 we introduce the general formulation of impulse response analysis, and introduce our multiple shock impulse response concept. Section 3 illustrates the properties of our concept using a first order vector autoregression model, and presents simulation studies. Section 4 presents the empirical application and Section 5 concludes.

2 Framework

Impulse response function (IRF) analysis allows the researcher to investigate the dynamic interactions, propagation, and persistence of shocks within a multivariate system of variables. We start by defining a general model to illustrate the impulse response concepts. Let $\boldsymbol{y}_t$ denote a vector containing n endogenous variables, modeled by the following general multivariate time series model

$$\boldsymbol{y}_t = f(\boldsymbol{y}_{t-1}, ..., \boldsymbol{y}_{t-p}, \boldsymbol{z}_t, ..., \boldsymbol{z}_{t-q}; \boldsymbol{\theta}_{1,t}) + g(\boldsymbol{u}_t; \boldsymbol{\theta}_{2,t}), \tag{1}$$

where $f(\cdot\,; \boldsymbol{\theta}_{1,t})$ denotes a specific functional form with predetermined, possibly time-varying, parameters $\boldsymbol{\theta}_{1,t}$ of the historical values of $\boldsymbol{y}_t$ up until lag p, and deterministic and/or exogenous variables $\boldsymbol{z}_t$ and its historical lagged values up until lag q. The function $g(\cdot\,; \boldsymbol{\theta}_{2,t})$ captures the dependencies between the n model residuals $\boldsymbol{u}_t$. The shocks have mean zero and finite variances. This general form allows for various model specifications, including both structural and reduced-form models, which can be linear or non-linear vector autoregression (VAR) models. It also encompasses dynamic factor models, non-linear factor models, and several regime-switching models like Markov-Switching, smooth transition, and stochastic volatility models. Furthermore, it allows for copula specifications on the error terms and GARCH specifications.

We first start by discussing the traditional and generalized IRFs. We then introduce the multiple shock impulse response functions.

2.1 Traditional Impulse Response Functions

Traditional IRFs can be used as a tool to answer the following question: *"What is the effect of a shock of size δ at time t on variables $\boldsymbol{y}_{t+h}$ at time $t+h$, given that no other shocks hit the system from time t until $t+h$?"*. In this paper, traditional impulse response functions refer to the following definition, as in Koop et al. (1996).

Definition 1 (**Traditional Impulse Response Functions**). *Let $\boldsymbol{y}_t$ follow a process in accordance with Equation* (1)*. The traditional impulse response functions of $\boldsymbol{y}_{t+h}$ to the s-th*

structural shock $\varepsilon_{s,t}$ *of size* δ_s *are defined as*

$$\begin{aligned}\boldsymbol{\Psi}^t(h, \varepsilon_{s,t} = \delta_s, \boldsymbol{\omega}_{t-1}) = \mathbb{E}[\boldsymbol{y}_{t+h} \mid \varepsilon_{s,t} = \delta_s, u_{j,t} = 0 \, \forall j \neq s, \boldsymbol{\varepsilon}_{t+1} = ... = \boldsymbol{\varepsilon}_{t+h} = \mathbf{0}, \boldsymbol{\omega}_{t-1}] \\ - \mathbb{E}[\boldsymbol{y}_{t+h} \mid \boldsymbol{\varepsilon}_t = \boldsymbol{\varepsilon}_{t+1} = ... = \boldsymbol{\varepsilon}_{t+h} = \mathbf{0}, \boldsymbol{\omega}_{t-1}], \end{aligned} \tag{2}$$

for horizon $h = 0, 1, ..., H$*, where* $\varepsilon_{s,t}$ *denotes the* s*-th element of the disturbances* $\boldsymbol{\varepsilon}_t$*, and* $\boldsymbol{\omega}_{t-1}$ *denotes an historical path realization of the stochastic process that generates* $\boldsymbol{y}_{t+h}$*.*

Thus, the traditional IRFs of $\boldsymbol{y}_{t+h}$ to the s-th shock $\varepsilon_{s,t}$ of size δ_s are the difference between two conditional expectations. The first conditional expectation measures the realization of $\boldsymbol{y}_{t+h}$ over time when the system is hit by a shock at time t, i.e., the perturbed realization. The second conditional expectation, often referred to as the benchmark, measures the realization of $\boldsymbol{y}_{t+h}$ when such a shock is absent.

As Koop et al. (1996) point out, the traditional IRF specification has certain properties that could be restrictive. The specification in Equation (2) implies that no other shocks take place at time t, and that there are no other shocks occurring from $t+1$ until $t+h$. Next to that, this specification conditions on a particular historical path of $\boldsymbol{y}_{t+h}$, denoted as $\boldsymbol{\omega}_{t-1}$. In order to be empirically useful, both the perturbed and benchmark realization need to be history independent, meaning that the historical path of the realization needs to be identical up until time $t-1$.

Traditional impulse response functions are primarily used in linear VAR models, as pioneered by Sims (1980). In these models, both $f(\cdot)$ and $g(\cdot)$ in Equation (1) follow linear specifications. The model's shocks, denoted as $\boldsymbol{u}_t$, are decomposed as $\boldsymbol{u}_t = \boldsymbol{C}\boldsymbol{\varepsilon}_t$, where the $n \times n$ matrix $\boldsymbol{C}$ describes the contemporaneous relationships among the structural shocks $\boldsymbol{\varepsilon}_t$. Sims (1980) linked these structural shocks to macroeconomic shocks, enabling the analysis of the impact of random impulses on a dynamic system. Subsequently, impulse response functions have become a widely adopted tool for examining dynamic relationships in multivariate linear systems. We elaborate on this in Section 3.1.

2.2 Generalized Impulse Response Functions

The specification of the traditional impulse response functions as in Definition 1 can be too restrictive in particular settings, such as non-linear or ambiguous underlying relations. Therefore, Koop et al. (1996) and Pesaran and Shin (1998) introduce the generalized impulse response function (GIRF) to treat these issues. The GIRF treats the impulse responses as a random variable itself in terms of historical paths and shocks. That is, the GIRF does not condition on a particular historical path and particular shock as in Equation (2), but rather on all possible histories and all possible shocks, or subsets of them.

The problem of the effect of possible future shocks occurring from $t+1$ until $t+h$ is dealt with by averaging them out, i.e., by taking the expectation over these future shocks. In this paper, we refer to the one shock generalized impulse response function as defined in the following definition.

Definition 2 (**Generalized Impulse Response Functions**). *Let $\boldsymbol{y}_t$ follow a process in accordance with Equation* (1)*. The generalized impulse response equivalent of the traditional impulse response functions $\boldsymbol{\Psi}^t(h, \varepsilon_{s,t} = \delta_s, \boldsymbol{\omega}_{t-1})$ defined in Definition 1 treats the history as random and conditions on the s-th shock of size δ_s. The one shock generalized impulse response functions of $\boldsymbol{y}_{t+h}$ to the s-th shock $u_{s,t}$ of size δ_s are defined as*

$$\boldsymbol{\Psi}^g(h, u_{s,t} = \delta_s, \mathcal{I}_{t-1}) = \mathbb{E}[\boldsymbol{y}_{t+h} \mid u_{s,t} = \delta_s, \mathcal{I}_{t-1}] - \mathbb{E}[\boldsymbol{y}_{t+h} \mid \mathcal{I}_{t-1}], \tag{3}$$

for horizon $h = 0, 1, ..., H$, where $u_{s,t}$ denotes the s-th element of the disturbances $\boldsymbol{u}_t$, and $\mathcal{I}_{t-1}$ denotes the non-decreasing information set available at $t-1$.

The main difference in this specification compared to the traditional IRF is that we do neither condition on other contemporaneous shocks nor assume future shocks to be zero, but rather integrate out these effects.

The GIRF defined in Equation (3) does not require explicit restrictions on the contemporaneous relations between the shocks. Instead, the generalized impulse response captures the effect of a system-wide shock, making it an attractive solution in case the causal relation between variables is ambiguous or when shocks are endogenous. Rambachan and Shephard

(2021) introduce a nonparametric, direct potential outcome system as a foundational framework for analyzing dynamic causal effects of assignments on outcomes in observational time series settings. Within this context, they explore the criteria that enable predictive time series estimands, such as orthogonalized and generalized IRFs, to be interpreted as dynamic causal effects of assignments on outcome variables. They highlight that the conditions for generalized impulse responses are considerably milder, without having to rely on orthogonalized error terms. In this context, the GIRF can be interpreted as the dynamic causal effect on the outcome variable.

2.3 Multiple Shock Impulse Response Functions

The generalized impulse response functions to one particular shock is given in Equation (3). However, in case of multiple shocks within a single period, possibly triggering one another, we need an alternative concept. Consider for example the financial crisis, where shocks from housing market collapses, banking disruptions, and credit contractions occurred simultaneously, all of which are interrelated within the economic framework. Additionally, during the COVID-19 pandemic, economies globally experienced simultaneous shocks from disrupted supply chains, plummeting consumer demand, and abrupt changes in monetary and fiscal policies, showcasing the interplay of multiple, interrelated variables. These events emphasize the complex interactions of variables, illustrating the need for a refined analytical tool.

The multiple shock impulse response function concept we introduce allows for analyzing the effect of m shocks from a set of variables occurring at time t, without making any assumptions on the underlying relation between these variables. We therefore introduce the concept of multiple shock impulse response functions, which is defined as follows.

Definition 3 (**Multiple Shock Impulse Response Functions**)**.** *Let $\boldsymbol{y}_t$ follow a process in accordance with Equation* (1)*. Let $\mathcal{S}$ be a set of indices corresponding to the locations of $m \leq n$ shocks of interest. The multiple shock impulse response functions treat the history as random, and condition on the set of m shocks of corresponding impulse sizes $\boldsymbol{\delta}_{\mathcal{S}}$. They are*

defined as the responses of $\boldsymbol{y}_{t+h}$ *to a set of shocks* $\boldsymbol{u}_{\mathcal{S},t}$ *of size* $\boldsymbol{\delta}_{\mathcal{S}}$*, i.e.,*

$$\boldsymbol{\Psi}^{\mathcal{S}}(h, \boldsymbol{u}_{\mathcal{S},t} = \boldsymbol{\delta}_{\mathcal{S}}, \mathcal{I}_{t-1}) = \mathbb{E}[\boldsymbol{y}_{t+h} \mid \boldsymbol{u}_{\mathcal{S},t} = \boldsymbol{\delta}_{\mathcal{S}}, \mathcal{I}_{t-1}] - \mathbb{E}[\boldsymbol{y}_{t+h} \mid \mathcal{I}_{t-1}], \tag{4}$$

for horizon $h = 0, 1, ..., H$*, where* $\boldsymbol{u}_{\mathcal{S},t}$ *denotes the subset the disturbances* $\boldsymbol{u}_t$*, and* $\mathcal{I}_{t-1}$ *denotes the non-decreasing information set available at* $t-1$*.*

In this definition, the impulse response shock size $\boldsymbol{\delta}_{\mathcal{S}}$ denotes an $m \times 1$ vector rather than a scalar δ_s in Definition 2. This definition allows for impulse response analysis of a set of shocks occur in the same period, without imposing restrictions on the structural relation between these shocks, and between the remaining shocks. It is a generalization of Definition 2 in terms of shocks of interest. In other words, when we consider $m = 1$ and select the s-th shock as the shock of interest, by setting $\mathcal{S} = \{s\}$, Definition 3 is equivalent to Definition 2.

Treating multiple shocks as one simultaneous assignment, the multiple shock impulse response functions align with the weaker conditions described in Rambachan and Shephard (2021). Consequently, these functions effectively quantify the dynamic causal effects of these simultaneous assignments on the outcome variables within a single time period.

Another property of the multiple shock impulse response function is that it takes into account the dependence between the shocks and corrects for this dependence while calculating the total effect of these shocks—treating them as one simultaneous assignment. Therefore, in case the m shocks of interest are all independent of each other, it holds that $\boldsymbol{\Psi}^{\mathcal{S}}(h, \boldsymbol{u}_{\mathcal{S},t} = \boldsymbol{\delta}_{\mathcal{S}}, \mathcal{I}_{t-1}) = \sum_{\ell \in \mathcal{S}} \boldsymbol{\Psi}^{g}(h, u_{\ell,t} = \delta_{\ell}, \mathcal{I}_{t-1})$. When the shocks of interest are dependent on each other, the simultaneous effect of these shocks cannot be calculated as the simple sum of their one shock GIRFs. For a dynamic causal interpretation, this approach fails since a key condition is the independence of assignments. In case of inherently independent shocks, the multiple shock impulse response functions are by definition the sum of the traditional impulse responses of the shocks of interest.

All IRF definitions mentioned above can be calculated using numerical methods. In the following section we illustrate the difference between the concepts using a simple linear vector autoregression model. This model allows for a closed-form solution of the conditional expectations and therefore an analytical solution for the impulse response functions, rather

than relying on numerical simulations.

3 A Linear Vector Autoregression Model

In order to illustrate the different concepts of IRFs described above, we consider a simple linear vector autoregression (VAR) process, conforming the general specification of Equation (1). Let $\boldsymbol{y}_t$ denote the n variables of interest. The VAR process with one lag is then[2]

$$\boldsymbol{y}_t = \boldsymbol{b} + \boldsymbol{B}\boldsymbol{y}_{t-1} + \boldsymbol{u}_t, \tag{5}$$

where $\boldsymbol{b}$ denotes the constant, $\boldsymbol{B}$ denotes the $n \times n$ coefficient matrix corresponding to the first lag and $\boldsymbol{u}_t$ denotes the reduced-form residuals. We make the following standard assumptions (see, e.g., Lütkepohl, 2005)

Assumption 1. *The residuals $\boldsymbol{u}_t$ of Equation (5) satisfy the following white noise conditions; (i) $\mathbb{E}[\boldsymbol{u}_t] = \boldsymbol{0}$, (ii) $\mathbb{E}[\boldsymbol{u}_t\boldsymbol{u}_t'] = \boldsymbol{\Sigma}$, for all t, where the covariance matrix $\boldsymbol{\Sigma}$ is positive definite and (iii) $\mathbb{E}[\boldsymbol{u}_t\boldsymbol{u}_v'] = \mathbf{O}_n$ for any $t \neq v$.*

Assumption 2. *The process of Equation (5) satisfies the stability condition. That is, all eigenvalues of $\boldsymbol{B}$ lie inside the unit circle, or equivalently, $\det(\boldsymbol{I}_n - \boldsymbol{B}\lambda) \neq 0$ for $|\lambda| < 1$.*

Here, $\boldsymbol{I}_n$ denotes the $n \times n$ identity matrix and $\mathbf{O}_n$ denotes the $n \times n$ zero matrix. Given that the VAR satisfies Assumption 2, there exists an infinite vector moving average (VMA) representation such that

$$\boldsymbol{y}_t = \boldsymbol{\mu} + \sum_{j=0}^{\infty} \boldsymbol{B}^j \boldsymbol{u}_{t-j}, \tag{6}$$

where $\boldsymbol{\mu} = (\boldsymbol{I}_n - \boldsymbol{B})^{-1}\boldsymbol{b}$ and $\boldsymbol{u}_t = \boldsymbol{y}_t - \mathbb{E}[\boldsymbol{y}_t \,|\, \mathcal{I}_{t-1}]$, such that the VMA is expressed in terms of reduced-form model residuals.

In the remainder of this section we state the traditional, one shock generalized and multiple shock impulse response functions in terms of the VAR(1) model. We then discuss the properties of these concepts, and their relation to each other. Finally, in two numerical

[2]For parsimony we consider a VAR(1) process with a constant. A VAR process with p lags can be written as a VAR(1) process using the companion form.

examples, we show the necessity of using multiple shock impulse response functions for accurately assessing the total effect of simultaneously occurring shocks, as opposed to merely summing individual impulse responses. Additionally, we highlight the value of this concept in mitigating potential temporal aggregation issues.

We consider the simple case of $\boldsymbol{y}_t$ containing $n = 3$ variables, such that $\boldsymbol{\Sigma}$ is a symmetric 3×3 matrix containing (co)variances σ_{ij} between variables i and j. We consider $m = 2$ shocks of interest, where we focus on shocks in the first two variables; $\mathcal{S} \in \{1, 2\}$. As the GIRF and multiple shock impulse response functions are order invariant, it does not matter which subset of shocks we choose to illustrate the difference between these two concepts. The traditional orthogonal impulse response functions assume a specific order of the variables. In this example we assume that the first two variables can contemporaneously affect the third variable.

3.1 Orthogonal Impulse Response Functions

In context of a linear VAR(1) model, we follow Definition 1. We use the VMA representation of Equation (6) and the mapping between the reduced-form residuals and the structural shocks; $\boldsymbol{u}_t = \boldsymbol{C}\boldsymbol{\varepsilon}_t$. Under Assumption 1–2, the traditional orthogonal impulse response functions of $\boldsymbol{y}_{t+h}$ to a structural shock $\varepsilon_{s,t}$ of size 1 are defined as[3]

$$\begin{aligned}\boldsymbol{\Psi}^t(h, \varepsilon_{s,t} = 1, \omega_{t-1}) = \; & \mathbb{E}[\boldsymbol{y}_{t+h} \mid \varepsilon_{s,t} = 1, \varepsilon_{j,t} = 0 \, \forall j \neq s, \boldsymbol{\varepsilon}_{t+1} = ... = \boldsymbol{\varepsilon}_{t+h} = \boldsymbol{0}, \boldsymbol{\omega}_{t-1}] \\ & - \mathbb{E}[\boldsymbol{y}_{t+h} \mid \boldsymbol{\varepsilon}_t = \boldsymbol{\varepsilon}_{t+1} = ... = \boldsymbol{\varepsilon}_{t+h} = \boldsymbol{0}, \boldsymbol{\omega}_{t-1}] \\ = \; & \boldsymbol{B}^h \boldsymbol{C} \boldsymbol{e}_s, \end{aligned} \tag{7}$$

for horizon $h = 0, 1, ..., H$. The selection or unit vector $\boldsymbol{e}_s$ is an $n \times 1$ vector for which all entries are 0 except entry s, which is 1. In a linear VAR, this IRF exhibits symmetry and proportionality: both positive and negative shocks yield equal effects, and a shock of size k produces k-fold the effect of a shock of size 1. Next to that, the traditional IRF is history independent, as it only depends on the coefficient matrix $\boldsymbol{B}$ and contemporaneous effects matrix $\boldsymbol{C}$.

[3] As a consequence, it holds that $\mathbb{E}[\boldsymbol{\varepsilon}_t] = \boldsymbol{0}$, $\mathbb{E}[\boldsymbol{\varepsilon}_t \boldsymbol{\varepsilon}_t'] = \boldsymbol{I}_n$ for all t and $\mathbb{E}[\boldsymbol{\varepsilon}_t \boldsymbol{\varepsilon}_v'] = \boldsymbol{O}_n$ for any $t \neq v$.

Note that the matrix $\boldsymbol{C}$ links the reduced-form residuals to the structural shocks. There are only $n(n-1)/2$ unknown parameters in the covariance matrix $\boldsymbol{\Sigma}$ of $\boldsymbol{u}_t$ due to its symmetry. However, $\boldsymbol{C}$ contains n^2 unknown parameters. The structural shocks are therefore not identified. Consequently, additional identifying restrictions need to be imposed. These restrictions are usually motivated by economic theory.[4]

The most popular assumption is to impose zero contemporaneous restrictions or recursive identification. The variables are ordered based on their assumed causal relations, i.e., we assume that some shocks have no contemporaneous effect on specific variables in the system. In practice, the variables that are ordered first drive the dynamics of the system, and the variables that are ordered last are the slower moving variables. The matrix $\boldsymbol{C}$ can be identified using the Cholesky decomposition of $\boldsymbol{\Sigma}$, representing the recursive structure.

Naturally, the impulse responses can be used to define the forecast error variance decomposition (FEVD) of the variables (see, e.g., Lütkepohl, 2005). This is the proportion of the h-step ahead forecast error variance of responding variable i to shock s. For a linear VAR, the FEVD denotes

$$\gamma_{i,s}^{t}(h) = \frac{\sum_{l=0}^{h} \left(\boldsymbol{e}_i' \boldsymbol{B}^l \boldsymbol{C} \boldsymbol{e}_s\right)^2}{\sum_{l=0}^{h} \boldsymbol{e}_i' \boldsymbol{B}^l \boldsymbol{\Sigma} (\boldsymbol{B}^l)' \boldsymbol{e}_i}, \tag{8}$$

for horizon $h = 0, ..., H$. The denominator corresponds to the total variance in the forecast error of variable i, and the numerator denotes the forecast error variance attributed to shock s. By construction, the FEVD sums up to one when summed over all shocks. The FEVD measures how much of the uncertainty in the forecast for a given variable is due to shocks to other variables in the system, and how much this evolves over time.

In our setting, we identify the contemporaneous relations by a Cholesky decomposition. We assume that variable 1 and 2 affect variable 3, but variable 3 does not affect 1 and 2 contemporaneously. In other words, variable 3 is a slow-moving variable. Therefore, summing the effect of shock 1 and 2 results in the following traditional impulse response functions

$$\sum_{s \in \mathcal{S}} \boldsymbol{\Psi}^t(h, \varepsilon_{s,t} = 1, \omega_{t-1}) = \boldsymbol{B}^h \boldsymbol{C}(\boldsymbol{e}_1 + \boldsymbol{e}_2) = \boldsymbol{B}^h \begin{bmatrix} c_{11} \\ c_{12} + c_{22} \\ c_{13} + c_{23} \end{bmatrix}, \tag{9}$$

[4]Examples of these restrictions are zero contemporaneous restrictions (Sims, 1980; Christiano et al., 1999), zero long-run restrictions (Blanchard and Quah, 1989; Gali, 1999), and sign restrictions (Uhlig, 2005).

where c_{ij} denotes the (i,j)-th element of matrix $\boldsymbol{C}$.

3.2 Generalized Impulse Response Functions

The key distinction between the traditional (orthogonal) impulse response functions and generalized impulse response functions lies in the treatment of shocks in the VAR. While the traditional IRFs involve an orthogonal decomposition of the reduced-form shocks, GIRFs employ a conditional expectation of the correlated shock to generate a unique reduced-form solution without imposing assumptions on the structural relations. In context of one lag linear VAR model, we need to impose normality on the residuals to obtain a closed-form solution (see, e.g., Koop et al., 1996; Pesaran and Shin, 1998).

Assumption 3. *The residuals* $\boldsymbol{u}_t$ *of Equation* (5) *are identically and independently normally distributed with mean* $\mathbf{0}$ *and covariance matrix* $\boldsymbol{\Sigma}$.

We follow Definition 2 and define the one shock generalized impulse response functions of $\boldsymbol{y}_{t+h}$ to the s-th shock $u_{s,t}$ of size δ_s. Similar to the traditional IRF, we use the VMA representation of the process $\boldsymbol{y}_{t+h}$ to work out the generalized impulse response functions. Under Assumption 1–3, allowing us to use the properties of the conditional expectations of the multivariate normal distribution, we obtain

$$\begin{aligned}\boldsymbol{\Psi}^g(h, u_{s,t} = \delta_s, \mathcal{I}_{t-1}) &= \mathbb{E}[\boldsymbol{y}_{t+h} \mid u_{s,t} = \delta_s, \mathcal{I}_{t-1}] - \mathbb{E}[\boldsymbol{y}_{t+h} \mid \mathcal{I}_{t-1}] \\ &= \boldsymbol{B}^h \boldsymbol{\Sigma} \boldsymbol{e}_s (\sigma_{ss})^{-1} \delta_s, \end{aligned} \tag{10}$$

for horizon $h = 0, 1, ..., H$. Again, $\boldsymbol{e}_s$ denotes the selection vector and σ_{ss} denotes the variance of shock s, i.e., the (s,s)-th entry of the covariance matrix $\boldsymbol{\Sigma}$.

To analyze the forecast error variance of variable i to shock s, we can also use the GIRF. The corresponding generalized FEVD (Koop et al., 1996) of variable i to shock s denotes

$$\gamma^g_{i,s}(h) = \frac{(\sigma_{ss})^{-1} \sum_{l=0}^{h} \left(\boldsymbol{e}_i' \boldsymbol{B}^l \boldsymbol{\Sigma} \boldsymbol{e}_s \right)^2}{\sum_{l=0}^{h} \boldsymbol{e}_i' \boldsymbol{B}^l \boldsymbol{\Sigma} (\boldsymbol{B}^l)' \boldsymbol{e}_i}, \tag{11}$$

for horizon $h = 0, ..., H$. Note that the denominator is the same as in Equation (8), as we

are using the same model and therefore the total variation in variable i does not change. The residuals are not orthogonal in this setting. Therefore, summing the generalized FEVD over the shocks for each variable i does not necessarily add up to 1.

The sum of the generalized impulse responses of Equation (10) corresponding to the first shock of size δ_1 and second shock of size δ_2 at horizon h is

$$\sum_{s\in\mathcal{S}} \boldsymbol{\Psi}^g(h, u_{s,t} = \delta_s, \mathcal{I}_{t-1}) = \boldsymbol{B}^h\Big(\boldsymbol{\Sigma}\boldsymbol{e}_1(\sigma_{11})^{-1}\delta_1 + \boldsymbol{\Sigma}\boldsymbol{e}_2(\sigma_{22})^{-1}\delta_2\Big) = \boldsymbol{B}^h \begin{bmatrix} \delta_1 + \frac{\sigma_{12}}{\sigma_{22}}\delta_2 \\ \frac{\sigma_{12}}{\sigma_{11}}\delta_1 + \delta_2 \\ \frac{\sigma_{13}}{\sigma_{11}}\delta_1 + \frac{\sigma_{23}}{\sigma_{22}}\delta_2 \end{bmatrix}. \quad (12)$$

According to this concept, the response of variable 1 (the first element) depends on the size of shock 1, corrected for the size of shock 2, taking into account the correlation between the two shocks. The same holds for variable 2. Therefore, this concept does not accurately represent the response of both variables to shock 1 and 2. The response of variable 3 does not depend on the correlation between the two shocks. This is a consequence of summing two single generalized impulse responses, where we condition on only one shock in each of the generalized impulse responses.

3.3 Multiple Shock Impulse Response Functions

Following Definition 3, we define the multiple shock impulse response functions for a linear VAR process. Under Assumption 1–3, we obtain a closed-form solution for the impulse response functions of m shocks at time t. The multiple shock impulse response function for m shocks is then

$$\begin{aligned} \boldsymbol{\Psi}^{\mathcal{S}}(h, \boldsymbol{u}_{\mathcal{S},t} = \boldsymbol{\delta}_{\mathcal{S}}, \mathcal{I}_{t-1}) =\ & \mathbb{E}[\boldsymbol{y}_{t+h} \mid \boldsymbol{u}_{\mathcal{S},t} = \boldsymbol{\delta}_{\mathcal{S}}, \mathcal{I}_{t-1}] - \mathbb{E}[\boldsymbol{y}_{t+h} \mid \mathcal{I}_{t-1}] \\ =\ & \boldsymbol{B}^h\boldsymbol{\Sigma}\boldsymbol{P}(\boldsymbol{P}'\boldsymbol{\Sigma}\boldsymbol{P})^{-1}\boldsymbol{\delta}_{\mathcal{S}}, \end{aligned} \quad (13)$$

where for the first expectation we use the VMA expression of Equation (A.1) and the properties of the conditional expectation of the multivariate normal distribution, such that

$$\begin{aligned}\mathbb{E}[\boldsymbol{y}_{t+h} \mid \boldsymbol{u}_{\mathcal{S},t} = \boldsymbol{\delta}_{\mathcal{S}}, \mathcal{I}_{t-1}] &= \boldsymbol{\mu} + \boldsymbol{B}^h \mathbb{E}[\boldsymbol{u}_t \mid \boldsymbol{u}_{\mathcal{S},t} = \boldsymbol{\delta}_{\mathcal{S}}, \mathcal{I}_{t-1}] + \sum_{j=1}^{\infty} \boldsymbol{B}^{h+j} \boldsymbol{u}_{t-j}, \\ &= \boldsymbol{\mu} + \boldsymbol{B}^h \boldsymbol{\Sigma} \boldsymbol{P} (\boldsymbol{P}' \boldsymbol{\Sigma} \boldsymbol{P})^{-1} \boldsymbol{\delta}_{\mathcal{S}} + \sum_{j=1}^{\infty} \boldsymbol{B}^{h+j} \boldsymbol{u}_{t-j}, \end{aligned} \tag{14}$$

where $\boldsymbol{P}$ denotes an $n \times m$ permutation matrix, containing m selection vectors where the selection indices correspond to the indices $\mathcal{S}$ of interest.

Similarly, we can define the forecast error variance of variable i that is assigned to the multiple simultaneous shocks $\mathcal{S}$. The multiple shock FEVD denotes

$$\gamma_i^{\mathcal{S}}(h) = \frac{\sum_{l=0}^{h} \boldsymbol{e}_i' \boldsymbol{B}^l \boldsymbol{\Sigma} \boldsymbol{P} (\boldsymbol{P}' \boldsymbol{\Sigma} \boldsymbol{P})^{-1} \boldsymbol{P}' \boldsymbol{\Sigma} (\boldsymbol{B}^l)' \boldsymbol{e}_i}{\sum_{l=0}^{h} \boldsymbol{e}_i' \boldsymbol{B}^l \boldsymbol{\Sigma} (\boldsymbol{B}^l)' \boldsymbol{e}_i}, \tag{15}$$

for horizon $h = 0, ..., H$. This multiple shock FEVD can be interpreted as a measure for the h-step ahead forecast error variance explained by the $\mathcal{S}$ shocks, thus, the percentage of unanticipated changes in variable i forecasts due to multiple shocks occurring simultaneously.

The propagation of the first two shocks in this linear example depends on $\boldsymbol{B}^h$. For the multiple shock impulse response functions, we have permutation matrix $\boldsymbol{P} = [\boldsymbol{e}_1, \boldsymbol{e}_2]$ and $\boldsymbol{\delta}_{\mathcal{S}} = [\delta_1, \delta_2]'$. Using Equation (13) we obtain

$$\boldsymbol{\Psi}^{\mathcal{S}}(h, \boldsymbol{u}_{\mathcal{S},t} = \boldsymbol{\delta}_{\mathcal{S}}, \mathcal{I}_{t-1}) = \boldsymbol{B}^h \begin{bmatrix} \delta_1 \\ \delta_2 \\ \frac{\sigma_{22}\sigma_{13} - \sigma_{12}\sigma_{23}}{\sigma_{11}\sigma_{22} - \sigma_{12}^2} \delta_1 + \frac{\sigma_{11}\sigma_{23} - \sigma_{12}\sigma_{13}}{\sigma_{11}\sigma_{22} - \sigma_{12}^2} \delta_2 \end{bmatrix}. \tag{16}$$

The j-th element of $\boldsymbol{\Psi}^{\mathcal{S}}$ corresponds to the response of variable j. The multiple shock impulse response function of variable 1 and 2 isolate the shocks coming from variable 1 and 2, respectively. The response of variable 3 to shocks in both 1 and 2 depend on the correlation between the shocks and variable 3, and corrects for the correlation between shock 1 and 2.

3.4 Comparing Impulse Response Functions

The traditional, one shock generalized and multiple shock impulse response functions can be linked to each other. The traditional IRFs are responses to a one standard deviation shock in the orthogonalized shock. By setting $\delta_s = \sqrt{\sigma_{ss}}$ in the GIRF we measure the effect of one deviation error shock. Thus, $\boldsymbol{\Psi}^g(h, u_{s,t} = \sqrt{\sigma_{ss}}, \mathcal{I}_{t-1})$ refers to the generalized impulse response functions to a one standard deviation shock. Equivalently, the multiple shock impulse responses to one standard deviation shocks in the m variables correspond to a shock size of $\boldsymbol{\delta}_{\mathcal{S}}$, containing the corresponding standard deviations to set $\mathcal{S}$. For a simultaneous shock in 1 and 2 this yields $\boldsymbol{\delta}_{\mathcal{S}} = \left[\sqrt{\sigma_{11}},\ \sqrt{\sigma_{22}}\right]'$. This is also referred to as the scaled impulse response functions.

Pesaran and Shin (1998) discuss the properties of the generalized impulse response functions in case the process $\boldsymbol{y}_t$ follows a multivariate linear model. Pesaran and Shin (1998) show that $\boldsymbol{\Psi}^t(h, \varepsilon_{s,t} = 1, \boldsymbol{\omega}_{t-1}) = \boldsymbol{\Psi}^g(h, u_{s,t} = \sqrt{\sigma_{ss}}, \mathcal{I}_{t-1})$, in case $\boldsymbol{\Sigma}$ is a diagonal matrix, i.e., when the reduced-form residuals $\boldsymbol{u}_t$ are uncorrelated. Further, in case when $\boldsymbol{\Sigma}$ is non-diagonal, the two impulse responses are the same for the first equation in the system. Let $\boldsymbol{\psi}_j^*(h, \cdot, \cdot) = \boldsymbol{e}_j' \boldsymbol{\Psi}^*(h, \cdot, \cdot)$ correspond to the j-th entry of the impulse response concept of interest. It holds that $\boldsymbol{\psi}_1^t(h, \varepsilon_{s,t} = 1, \boldsymbol{\omega}_{t-1}) = \boldsymbol{\psi}_1^g(h, u_{s,t} = \sqrt{\sigma_{ss}}, \mathcal{I}_{t-1})$. One could therefore calculate the generalized impulse response of a shock in variable j by ordering this variable first and calculating the traditional impulse response function using the Cholesky decomposition.

A feature of the multiple shock impulse response functions is that it takes into account the correlation between the shocks of interest. In case the shocks of interest are uncorrelated to each other, we find that the sum of generalized IRFs is equivalent to the multiple shock impulse response functions. For example, in our considered case $\mathcal{S} = \{1, 2\}$, it is easy to see that for $\sigma_{12} = 0$, Equation (12) and Equation (16) yield the same expression. Further, the sum of the scaled generalized and scaled multiple shock IRFs are equivalent to the sum of the traditional IRFs.

3.5 Numerical Examples

We consider two simulation studies to illustrate the differences between the various impulse response function concepts. In the first setting we show the need for the multiple shock impulse response functions in order to accurately analyze the total effect of multiple shocks, and in the second setting we show that the multiple shock impulse response functions can be helpful in order to overcome temporal aggregation issues.

3.5.1 Properties of the Impulse Response Concepts

The aim of this study is to shed light on the behavior of the impulse response functions in case of multiple simultaneous shocks. We consider the most simple form of Equation (5); we set the constant to zero, and consider $n = 3$ endogenous variables. The data generating process (DGP) is

$$\boldsymbol{y}_t = \boldsymbol{B}\boldsymbol{y}_{t-1} + \boldsymbol{u}_t, \qquad \boldsymbol{u}_t \sim N(\boldsymbol{0}, \boldsymbol{\Sigma}), \tag{17}$$

where

$$\boldsymbol{B} = \begin{bmatrix} 0.4 & 0.1 & 0.1 \\ 0.1 & 0.4 & 0.1 \\ 0.2 & 0.2 & 0.4 \end{bmatrix} \qquad \text{and} \qquad \boldsymbol{\Sigma} = \begin{bmatrix} \sigma_{11} & \sigma_{12} & \sigma_{13} \\ \sigma_{12} & \sigma_{22} & \sigma_{23} \\ \sigma_{13} & \sigma_{23} & \sigma_{33} \end{bmatrix}. \tag{18}$$

We examine four different parameterizations of the covariance matrix $\boldsymbol{\Sigma}$, as shown in Table 1. Recall that we focus on $m = 2$ one standard deviation shocks shocks of interest, with locations $\mathcal{S} \in \{1, 2\}$. The ordering of variables is only relevant for the traditional impulse response functions, for which we assume that both shocks can contemporaneously affect the third variable.

In order to numerically show the differences between the multiple shock impulse responses of Equation (16), summing the generalized impulse responses of Equation (12) and summing the traditional impulse responses of Equation (9). Figure 1 shows the multiple shock impulse response functions and the generalized impulse response functions corresponding to these four specifications. In all figures, the solid dark blue star marked lines correspond to the multiple shock impulse response function of $y_{3,t}$ to shock 1 and 2, the light blue lines correspond to the individual one shock GIRF of $y_{3,t}$ to shock 1 and 2, respectively. The solid red cross marked lines are the sum of these generalized impulse response functions, and the solid yellow plus

Table 1: DGP parameter settings of Equation (17)

	Specification	Description
1.	$\boldsymbol{\Sigma}^{(1)} = \begin{bmatrix} 1 & 0.25 & 0.1 \\ 0.25 & 1 & 0.5 \\ 0.1 & 0.5 & 1 \end{bmatrix}$	Shock 1 and 2 covariance is positive ($\sigma_{12} > 0$), and shock covariance of 1 and 2 to 3 is positive ($\sigma_{13}, \sigma_{23} > 0$).
2.	$\boldsymbol{\Sigma}^{(2)} = \begin{bmatrix} 1 & -0.25 & 0.1 \\ -0.25 & 1 & 0.5 \\ 0.1 & 0.5 & 1 \end{bmatrix}$	Shock 1 and 2 covariance is negative ($\sigma_{12} < 0$), and shock covariance of 1 and 2 to 3 is positive ($\sigma_{13}, \sigma_{23} > 0$).
3.	$\boldsymbol{\Sigma}^{(3)} = \begin{bmatrix} 1 & 0.25 & -0.1 \\ 0.25 & 1 & 0.5 \\ -0.1 & 0.5 & 1 \end{bmatrix}$	Shock 1 and 2 covariance is positive ($\sigma_{12} > 0$), and shock covariance of 1 and 2 to 3 is negative and positive, respectively ($\sigma_{13} < 0, \sigma_{23} > 0$).
4.	$\boldsymbol{\Sigma}^{(4)} = \begin{bmatrix} 1 & 0 & 0.1 \\ 0 & 1 & 0.5 \\ 0.1 & 0.5 & 1 \end{bmatrix}$	Shock 1 and 2 covariance is zero ($\sigma_{12} = 0$), and shock covariance of 1 and 2 to 3 is positive ($\sigma_{13}, \sigma_{23} > 0$).

Note: Our illustration focuses on the effect of a simultaneous shock in variable 1 and 2 on variable 3.

marked lines are the sum of the traditional impulse response functions. Note that for the traditional IRFs, we identify the contemporaneous relations using a Cholesky decomposition.

Figure 1 shows that the degree of over- and underestimation of the generalized impulse response functions is contingent upon the data generating process, and is therefore non-trivial to estimate a priori. In specification 1, where the covariance between the shocks of interest $\mathcal{S}$ is positive, the sum of the GIRFs and traditional IRFs overestimate the effect of both shocks, whereas for the case of negative covariance between the first and second shock (specification 2), the sum of both underestimate the total effect. The third specification, showing the case of negative and positive covariance of variable 3 to 1 and 2, is quite similar to specification 1. However, the degree of overestimation of the sum of the GIRFs at $h = 0$ is mitigated by the negative covariance between variable 1 and 3 compared to specification 1. For $h > 0$ the degree of overestimation is roughly similar to specification 1. The degree of over- and underestimation also depends on the correlation strength between the shocks of interest—when the strength increases in absolute terms, the difference between the multiple shock impulse response functions and sum of the GIRFs becomes larger. Specification 4 shows the equivalence of the sum of GIRFs, the sum of traditional IRFs and multiple shock impulse response functions described in Section 3.4 in case the shocks of interest are uncorrelated.

Figure 1: Impulse response concepts for four DGP specifications

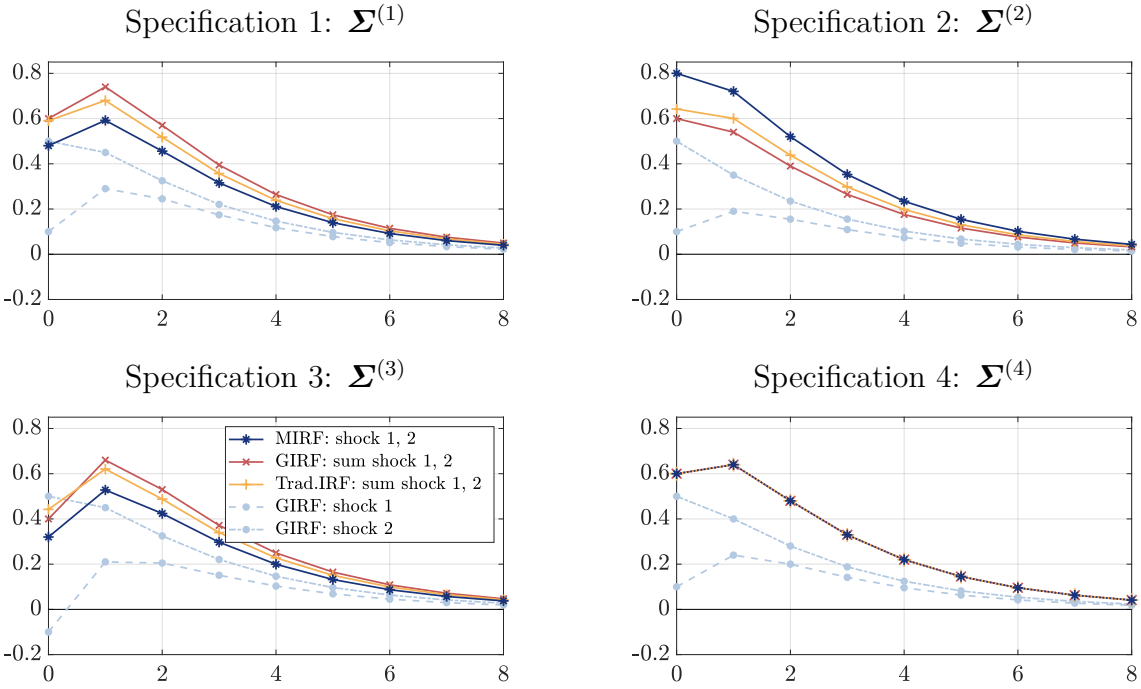

Note: The DGP specifications are given in Table 1. All impulse responses correspond to the response of variable 3 to one standard deviation shocks. The solid dark blue lines with star markers correspond to the multiple shock impulse response functions of shock 1 and 2. The solid red (cross markers) and yellow lines (plus markers) correspond to the sum of the generalized and traditional impulse response functions to shock 1 and 2, respectively. The dashed and dashed-dotted light blue lines correspond to the one shock generalized impulse response functions of shock 1 and 2, respectively.

3.5.2 Mixed Frequency and Temporal Aggregation

In the context of multiple shocks occurring, multiple shock impulse response functions can be helpful in mitigating potential temporal aggregation issues. To illustrate this, we use the framework of Ghysels (2016).[5] The set up is similar to their numerical illustration in section 6. We consider two frequencies. Let $\{\boldsymbol{y}_t : t = 1, ..., T\}$ denote the n variables sampled at the lowest frequency. Let $\{\ddot{\boldsymbol{y}}(t, j) : t = 1, ..., T, j = 1, ..., m\}$ denote the n variables sampled m times during period t, denoting the latent multivariate high-frequency process $\ddot{\boldsymbol{y}}(t)$. As before, we consider $n = 3$ variables and set the sampling frequency at $m = 4$, reflecting a sample difference of weekly versus monthly data, where we assume that there are four weeks

[5]They introduce a mixed frequency VAR framework, where high- and low frequency variables are stacked into one encompassing VAR model. This stacked skip-sampled approach is a multivariate extension of mixed-data sampling (MIDAS) regressions of Ghysels et al. (2004, 2007). In this research, we merely consider the latent stacked high frequency process and the aggregated process.

in one month. We assume that we do not observe the high frequency process. The latent higher frequency process is

$$\ddot{\boldsymbol{y}}(t) = \Big[\ddot{y}_1(t,1),\ \ddot{y}_2(t,1),\ \ddot{y}_3(t,1),\ \ddot{y}_1(t,2),\ \ddot{y}_2(t,2),\ \ddot{y}_3(t,2),\ \ddot{y}_1(t,3),\ \ddot{y}_2(t,3),\ \ddot{y}_3(t,3),\ \ddot{y}_1(t,4),\ \ddot{y}_2(t,4),\ \ddot{y}_3(t,4)\Big]'. \tag{19}$$

Our DGP is a VAR(1) model of the $k = n \times m$ dimensional latent process with no constant. The DGP is a stacked version of a regular high frequency weekly VAR(1) model and has the following structure

$$\begin{bmatrix} \boldsymbol{A}_0^{1,1} & \mathbf{O}_3 & \mathbf{O}_3 & \mathbf{O}_3 \\ -\boldsymbol{A}_0^{2,1} & \boldsymbol{A}_0^{2,2} & \mathbf{O}_3 & \mathbf{O}_3 \\ \mathbf{O}_3 & -\boldsymbol{A}_0^{3,2} & \boldsymbol{A}_0^{3,3} & \mathbf{O}_3 \\ \mathbf{O}_3 & \mathbf{O}_3 & -\boldsymbol{A}_0^{4,3} & \boldsymbol{A}_0^{4,4} \end{bmatrix} \ddot{\boldsymbol{y}}(t) = \begin{bmatrix} \mathbf{O}_3 & \mathbf{O}_3 & \mathbf{O}_3 & \boldsymbol{A}^{1,4} \\ \mathbf{O}_3 & \mathbf{O}_3 & \mathbf{O}_3 & \mathbf{O}_3 \\ \mathbf{O}_3 & \mathbf{O}_3 & \mathbf{O}_3 & \mathbf{O}_3 \\ \mathbf{O}_3 & \mathbf{O}_3 & \mathbf{O}_3 & \mathbf{O}_3 \end{bmatrix} \ddot{\boldsymbol{y}}(t-1) + \ddot{\boldsymbol{\varepsilon}}(t), \quad \ddot{\boldsymbol{\varepsilon}}(t) \sim \mathcal{N}(\mathbf{0}, \mathbf{I}_k), \tag{20}$$

where we set

$$\boldsymbol{A}_0^{2,1} = \boldsymbol{A}_0^{3,2} = \boldsymbol{A}_0^{4,3} = \boldsymbol{A}^{1,4} = \begin{bmatrix} 0.4 & 0.1 & 0.1 \\ 0.1 & 0.4 & 0.1 \\ 0.2 & 0.2 & 0.4 \end{bmatrix}. \tag{21}$$

The error term $\ddot{\boldsymbol{\varepsilon}}(t)$ has the same stacked structure as Equation (19).

In line with Ghysels (2016), we set the persistence to 0.4, which is a moderate persistence in the time series and we set the dependency between variables to be low, i.e., 0.1 and 0.2, representative for macro and financial time series data. We consider four different specifications for $\boldsymbol{A}_0^{j,j}$ for $j = 1, 2, 3, 4$, which capture the contemporaneous relations between the variables on the higher frequency. This DGP structure imposes dependency of the high frequency data on both the high- and low frequency data, and dependency of the low frequency data on both the high- and low frequency data. We set $T = 240$ months, a representative sample size in economic settings. We report results based on 1000 draws.

We focus on the effect of a shock in variable 1 in the first month with a shock in variable 2 taking place in the second month, on variable 3. In order to identify these shocks in the stacked latent DGP, we use the lower triangular Cholesky factorization to identify shocks, as it takes into account the natural order in this mixed frequency framework with the variables being ordered as in Equation (19). As a result, the identified shocks are orthogonal to each

other. Therefore, the effect of the two (higher frequency) shocks is just the sum of these impulse responses, that is, $\ddot{\boldsymbol{\Psi}}^t(h, \ddot{\varepsilon}_1(t,1) = 1, \boldsymbol{\omega}_{t-1}) + \ddot{\boldsymbol{\Psi}}^t(h, \ddot{\varepsilon}_2(t,2) = 1, \boldsymbol{\omega}_{t-1})$. We sum the effect of these two shocks over the responding variables $\ddot{y}_3(t,1)$, $\ddot{y}_3(t,2)$, $\ddot{y}_3(t,3)$ and $\ddot{y}_3(t,4)$ in order to obtain the total effect on the aggregated $y_{3,t}$.

Recall that the researcher does not observe the latent high frequency DGP. Instead, the researcher observes a low frequency process $\boldsymbol{y}_t = \begin{bmatrix} y_{1,t}, & y_{2,t}, & y_{3,t} \end{bmatrix}'$, also referred to as the aggregated process. The aggregated process is linked to the latent process with the following aggregation scheme

$$\boldsymbol{y}_t = \begin{bmatrix} 1 & 0 & 0 & 1 & 0 & 0 & 1 & 0 & 0 & 1 & 0 & 0 \\ 0 & 1 & 0 & 0 & 1 & 0 & 0 & 1 & 0 & 0 & 1 & 0 \\ 0 & 0 & 1 & 0 & 0 & 1 & 0 & 0 & 1 & 0 & 0 & 1 \end{bmatrix} \ddot{\boldsymbol{y}}(t). \tag{22}$$

We consider the VAR(1) process of Equation (5) (without a constant) for the aggregated low frequency process $\boldsymbol{y}_t$. We estimate these reduced-form parameters with OLS.

In the low frequency framework a shock in variable 1 in the first month with a shock in variable 2 in the second month corresponds to a shock in variable 1 and 2 simultaneously at time t. We calculate the sum of the traditional impulse responses to one standard deviation shocks using Equation (9), the sum of the generalized impulse responses using Equation (12), and the multiple shock impulse response functions using Equation (16), where for the generalized and multiple shock impulse responses we consider $\delta_1 = \sqrt{\sigma_{11}}$ and $\delta_2 = \sqrt{\sigma_{22}}$. We further scale the shock size of these aggregated impulse response functions by $1/\sqrt{4}$ to compare the magnitude to the magnitude of the DGP.[6]

Figure 2 shows the impulse responses for our DGP specifications. All solid lines are based on aggregated data. The solid dark lines correspond to the median multiple shock IRFs, the yellow and red solid lines correspond to the median traditional and generalized IRFs, respectively. The dashed dotted lines correspond to the impulse response functions originating from true underlying mixed frequency DGP. In all specifications, the traditional and generalized IRFs overestimate the true effect. The first specification shows no contemporaneous relation

[6]Note that this scaling is not completely accurate, as it relies on the assumption that the observations within the higher frequency interval are i.i.d., which is inherently not the case in our DGP specifications 2–4.

Table 2: DGP parameter settings of Equation (20)

	Specification for $j = 1, 2, 3, 4$	Description
1.	$\boldsymbol{A}_0^{j,j(1)} = \begin{bmatrix} 1 & 0 & 0 \\ 0 & 1 & 0 \\ 0 & 0 & 1 \end{bmatrix}$	No contemporaneous relation at higher frequency (within same month). Structure as in Ghysels (2016).
2.	$\boldsymbol{A}_0^{j,j(2)} = \begin{bmatrix} 1 & -0.1 & -0.1 \\ -0.1 & 1 & -0.1 \\ -0.1 & -0.1 & 1 \end{bmatrix}$	Contemporaneous relation at higher frequency between all three variables is positive.
3.	$\boldsymbol{A}_0^{j,j(3)} = \begin{bmatrix} 1 & 0.1 & -0.1 \\ 0.1 & 1 & -0.1 \\ -0.1 & -0.1 & 1 \end{bmatrix}$	Contemporaneous relation at higher frequency between variable 1 and 2 is negative, and the relation of variable 1 and 2, to 3 is positive.
4.	$\boldsymbol{A}_0^{j,j(4)} = \begin{bmatrix} 1 & -0.1 & 0.1 \\ -0.1 & 1 & -0.1 \\ 0.1 & -0.1 & 1 \end{bmatrix}$	Contemporaneous relation at higher frequency between variable 1 and 2 is positive, and the relation of variable 1 (2) to 3 is negative (positive).

Note: Our illustration focuses on the effect of a simultaneous shock in variable 1 in the first month, and variable 2 in the second month, on variable 3. Note that the off-diagonal elements of $\boldsymbol{A}_0^{j,j}$ have opposite signs, as $\boldsymbol{A}_0$ is on the left-hand side of Equation (20).

between the variables at the highest frequency, but a positive lagged relation between the variables at higher frequency. Specifications 2–4 show various contemporaneous correlation structures between the variables. In general, the multiple shock impulse response functions most closely resemble the true underlying DGP impulse responses—showing their potential to overcome temporal aggregation in case of multiple shocks.

Figure 2: Impulse response concepts for four latent DGP specifications

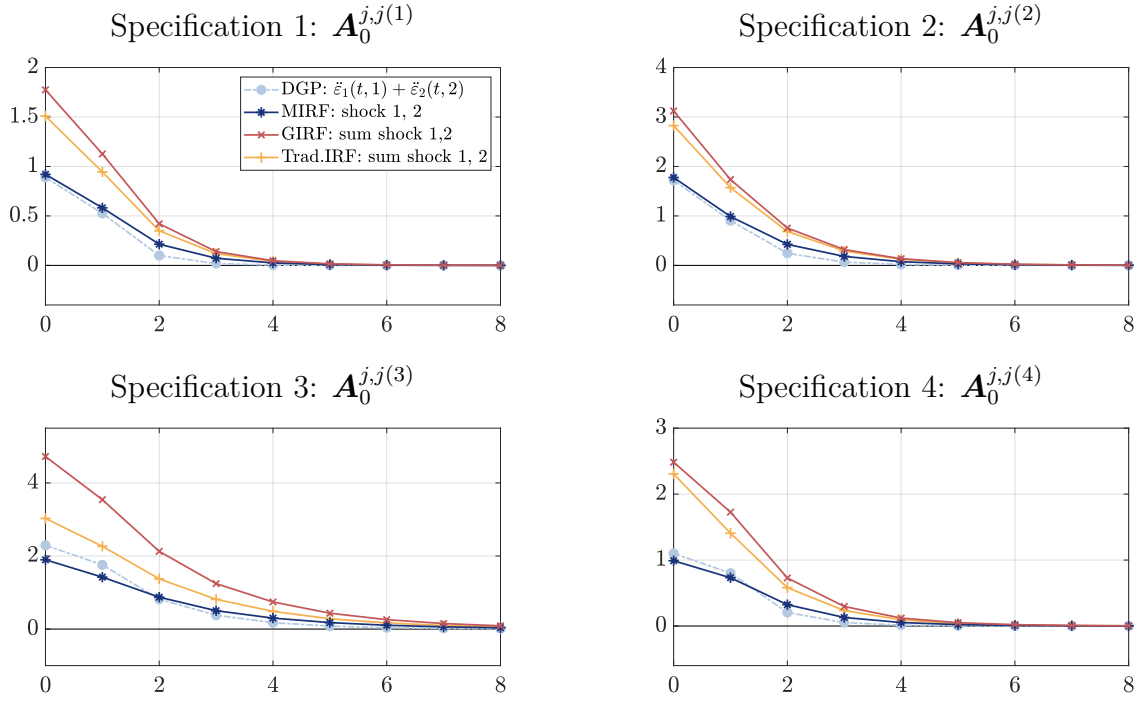

Note: The DGP specifications are given in Table 2. All impulse responses correspond to the response of variable 3 to one standard deviation shocks (in the latent process). This corresponds to a shock correction of $1/\sqrt{m}$ in the aggregated process. The x-axis corresponds to the horizon at the aggregated lower frequency. The dashed-dotted light blue line corresponds to the impulse response function to a shock in variable 1 in the first week, and a shock in variable 2 in the second week, originated from the latent (unobserved) DGP. The solid dark blue line with star markers corresponds to the multiple shock impulse response functions of shock 1 and 2. The solid red (cross markers) and yellow lines (plus markers) correspond to the sum of the generalized and traditional impulse response functions to shock 1 and 2, respectively. The aggregated IRFs are median responses over 1000 simulations for $T = 240$.

4 Multiple Shocks in the Interconnected Euro Area

During the European debt crisis, monetary policy tightening by the European Central Bank (ECB) to address the upward inflation path intensified financial uncertainty in already vulnerable Euro area countries such as Greece, Italy, Portugal, and Spain. See Rostagno et al. (2019) section 4.8 for an in depth discussion. This monetary tightening, combined with pre-existing vulnerabilities of the EMU, exacerbated financial uncertainty and instability (Lane, 2012). Rising borrowing costs, decline in market confidence, and interdependencies within the financial system amplified the effects,[7] leading to heightened market volatility, increased risk premiums, and risk aversion among investors.

[7] Beirne and Fratzscher (2013) find evidence of herding behavior in sovereign yields during the debt crisis.

In this application, we focus on two types of shocks. First, we examine the transmission of these monetary policy shocks, simultaneous with uncertainty shocks in lower credit rating countries. The rationale for considering multiple shocks for different shock types is rooted in the complex and intertwined nature of financial markets. Different shock types can have overlapping, reinforcing, or counteracting effects on economies, especially during turbulent periods. By analyzing multiple model shocks, we aim to capture a more comprehensive picture of the potential interactions and chain effects that can arise in real-world scenarios. Especially during turbulent economic times, these shocks can swiftly shift the perceived risk among borrowers and lenders, affecting their outlook on systematic risk in financial markets. These shocks tend to take place within a month, a time frame that often represents the finest granularity in macroeconomic data sets. This illustrates the need for a framework designed to assess the impacts of multiple concurrent shocks within a single period, addressing potential challenges related to temporal aggregation. Second, we examine the transmission of a negative shock to equity prices in all countries combined as a proxy for an area-wide shock, and show the usefulness of the multiple shock impulse response functions in this context compared to a GDP-weighted average of country-specific equity shocks, as done in literature.

We consider four countries, France, Germany, Italy, and Spain, as these are the four largest economies in the Euro zone contributing to over 70% of the Euro zone GDP over our sample. These four countries also capture the heterogeneity within Europe in terms of solvency.[8] We analyze the effect of a monetary policy shock combined with uncertainty shocks in Italy and Spain, as well as the effect of a European-wide equity shock. Our monthly data ranges from January 1999 until October 2022.

4.1 Global Vector Autoregression Framework

We consider the global vector autoregression (GVAR) framework introduced in Pesaran et al. (2004) and extended by Dees et al. (2007), for four Euro area countries. Each country's economy is modeled by a domestic VAR, and common Euro area (monetary) factors are

[8]During our sample period, France's credit rating is considered high grade (AA-AAA), Germany's rating is considered prime (AAA), Italy is considered lower medium grade (about BBB) and Spain is considered medium grade (BBB-A), according to Moody's, S&P and Fitch. See https://countryeconomy.com/ratings.

modeled in a separate VAR. The framework allows for modeling direct effects of Euro area and country-specific shocks, and for modeling cross-country interactions.

Let $\boldsymbol{y}_{i,t}$ be a $k_i \times 1$ vector containing variables corresponding to country i. We assume there are N countries, and for each country i there are k_i^* foreign variables $\boldsymbol{y}_{i,t}^*$ with country-specific weights and k_x common global variables $\boldsymbol{x}_t$. The domestic variables of country i follow a VARX(p_i) process

$$\boldsymbol{y}_{i,t} = \boldsymbol{c}_i + \sum_{\ell=1}^{p_i} \boldsymbol{C}_{i,\ell} \boldsymbol{y}_{i,t-\ell} + \sum_{\ell=0}^{q_i} \boldsymbol{\Lambda}_{i,\ell} \boldsymbol{y}_{i,t-\ell}^* + \boldsymbol{\Gamma}_{i,0} \boldsymbol{x}_t + \boldsymbol{\eta}_{i,t}, \tag{23}$$

where $\boldsymbol{c}_i$ denotes the intercept, $\boldsymbol{C}_{i,\ell}$ are $k_i \times k_i$ coefficient matrices of the lagged endogenous variables, $\boldsymbol{\Lambda}_{i,\ell}$ are $k_i \times k_i^*$ coefficient matrices of the foreign-specific variables $\boldsymbol{y}_{i,t-\ell}^*$, and $\boldsymbol{\Gamma}_{i,0}$ are $k_i \times k_x$ coefficient matrices corresponding to the common global variables $\boldsymbol{x}_t$. We assume that the idiosyncratic country-specific shocks $\boldsymbol{\eta}_{it}$ are serially uncorrelated with zero mean and variance-covariance matrix $\boldsymbol{\Sigma}_{i,i}$.

The foreign-specific variables capture the relative impact of spillover effects between countries. Specifically, they are a trade-weighted sum of the variables of the other countries, such that

$$\boldsymbol{y}_{i,t}^* = \sum_{j=1, j\neq i}^{N} w_{i,j} \boldsymbol{y}_{j,t}, \quad \text{with} \quad \sum_{j=1, j\neq i}^{N} w_{i,j} = 1, \tag{24}$$

for every country i. The common global variables $\boldsymbol{x}_t$ follow a VARX(p_x, q_x) process

$$\boldsymbol{x}_t = \boldsymbol{c}_x + \sum_{\ell=1}^{p_x} \boldsymbol{\Theta}_\ell \boldsymbol{x}_{t-\ell} + \sum_{\ell=0}^{q_x} \boldsymbol{\Phi}_\ell \widetilde{\boldsymbol{y}}_{t-\ell} + \boldsymbol{\eta}_{x,t}, \tag{25}$$

where $\boldsymbol{c}_x$ is the intercept, and $\boldsymbol{\Theta}_\ell$ and $\boldsymbol{\Phi}_\ell$ are coefficient matrices. The exogenous $\widetilde{k} \times 1$ vector $\widetilde{\boldsymbol{y}}_t$ measures the Euro area economy, which is a GDP-weighted average of the domestic variables such that

$$\widetilde{\boldsymbol{y}}_t = \sum_{j=1}^{N} \widetilde{w}_j \boldsymbol{y}_{j,t}, \quad \text{with} \quad \sum_{j=1}^{N} \widetilde{w}_j = 1. \tag{26}$$

The GVAR framework allows for cross-country interactions through linkages by foreign-specific variables in Equation (23), non-zero contemporaneous dependence of shocks, e.g., $\boldsymbol{\Sigma}_{i,j} \neq 0$ for country i and j, and common Euro area factors. Exploiting that $\boldsymbol{y}_{i,t}^*$ and $\widetilde{\boldsymbol{y}}_t$ are

both linear combinations of the country-specific variables $\boldsymbol{y}_{i,t}$, we can combine Equation (23) and Equation (25) into one model, such that

$$\boldsymbol{H}_0 \boldsymbol{z}_t = \boldsymbol{h}_0 + \sum_{\ell=1}^{p^*} \boldsymbol{H}_\ell \boldsymbol{z}_{t-\ell} + \boldsymbol{\varepsilon}_t, \tag{27}$$

where $p^* = \max(p, q, q_x)$, $\boldsymbol{z}_t = [\boldsymbol{x}_t', \boldsymbol{y}_t']'$, $\boldsymbol{h}_0 = [\boldsymbol{c}_x', \boldsymbol{c}']'$ and the residuals $\boldsymbol{\varepsilon}_t = [\boldsymbol{\eta}_{x,t}', \boldsymbol{\eta}_t']'$, with variance-covariance matrix $\boldsymbol{\Sigma}_e$. Provided that $\boldsymbol{H}_0$ is invertible, we obtain the reduced-form model

$$\boldsymbol{z}_t = \boldsymbol{k}_0 + \sum_{\ell=1}^{p^*} \boldsymbol{K}_\ell \boldsymbol{z}_{t-\ell} + \boldsymbol{u}_t, \tag{28}$$

where $\boldsymbol{k}_0 = \boldsymbol{H}_0^{-1}\boldsymbol{h}_0$, $\boldsymbol{K}_\ell = \boldsymbol{H}_0^{-1}\boldsymbol{H}_\ell$, and $\boldsymbol{u}_t = \boldsymbol{H}_0^{-1}\boldsymbol{\varepsilon}_t$ with $\mathbb{E}[\boldsymbol{u}_t \boldsymbol{u}_t'] = \boldsymbol{H}_0^{-1}\boldsymbol{\Sigma}_\varepsilon\Big(\boldsymbol{H}_0^{-1}\Big)' = \boldsymbol{\Sigma}_u$. Here, $\boldsymbol{H}_0^{-1}$ captures the contemporaneous relations between the structural shocks $\boldsymbol{\varepsilon}_t$. To obtain this result, we impose the following assumptions.

Assumptions (Global VAR). *(i) The residuals $\boldsymbol{\eta}_{i,t}$ of Equation (23) and $\boldsymbol{\eta}_{x,t}$ of Equation (25) are assumed to be serially uncorrelated with zero mean and variance-covariance matrix $\boldsymbol{\Sigma}_{i,i}$ and $\boldsymbol{\Sigma}_{x,x}$, respectively. (ii) The trade-based weights $w_{i,j}$ in Equation (24) are constant over time. (iii) Equation (28) satisfies the stability condition described in Assumption 2. (iv) The foreign-specific variables in Equation (23) are assumed to be weakly exogenous.*

The last assumption (iv) is necessary in order to estimate the model parameters in a country-per-country setting. Given the reduced-form in Equation (28), we can calculate the traditional, generalized, and multiple impulse response functions for horizon $h = 1, ..., H$ in a similar way by the following recursion

$$\boldsymbol{\Psi}^*(h, \cdot, \cdot) = \sum_{l=1}^{h} \boldsymbol{\Psi}^*(h-l, \cdot, \cdot)\boldsymbol{K}_l, \tag{29}$$

where $\boldsymbol{K}_l = 0$ in case $l > p^*$. The initial conditions are as follows: $\boldsymbol{\Psi}^t(0, \varepsilon_{s,t} = 1, \omega_{t-1}) = \boldsymbol{C}\boldsymbol{e}_s$, $\boldsymbol{\Psi}^g(0, u_{s,t} = \delta_s, \mathcal{I}_{t-1}) = \boldsymbol{\Sigma}_u \boldsymbol{e}_s (\sigma_{ss})^{-1}\delta_s$ and $\boldsymbol{\Psi}^{\mathcal{S}}(0, \boldsymbol{u}_{\mathcal{S},t} = \boldsymbol{\delta}_{\mathcal{S}}, \mathcal{I}_{t-1}) = \boldsymbol{\Sigma}_u \boldsymbol{P}(\boldsymbol{P}'\boldsymbol{\Sigma}_u\boldsymbol{P})^{-1}\boldsymbol{\delta}_{\mathcal{S}}$, where shock sizes δ_s and $\boldsymbol{\delta}_{\mathcal{S}}$ are set to one standard deviation shocks.

The traditional and general impulse response functions focus on a single shock. However,

not all shocks are tied to a single country. Global or area-wide shocks, like technological advancements or broad market shifts, affect the entire world economy. Dees et al. (2007) define the generalized impulse responses to one standard error global or regional shock as a GDP-weighted average of the specific-variable shocks from the considered countries in the region. That is,

$$\boldsymbol{\Psi}^g\left(h, u^r_{s,t} = \sqrt{\boldsymbol{w}_s'\boldsymbol{\Sigma}_u\boldsymbol{w}_s}, \mathcal{I}_{t-1}\right) = \frac{\boldsymbol{G}_h\boldsymbol{\Sigma}_u\boldsymbol{w}_s}{\sqrt{\boldsymbol{w}_s'\boldsymbol{\Sigma}_u\boldsymbol{w}_s}}, \tag{30}$$

where $\boldsymbol{w}_s$ is a selection vector where every element is zero, except for the element corresponding to the s-th variable. This specific element is set equal to $\widetilde{w}_i$, representing the GDP weight of the i-th country in the global economy as in Equation (26). The coefficient matrix $\boldsymbol{G}_h$ is derived through the recursive formula provided below, initialized with $\boldsymbol{G}_0 = \boldsymbol{I}$:

$$\boldsymbol{G}_l = \boldsymbol{K}_1\boldsymbol{G}_{l-1} + ... + \boldsymbol{K}_{p^*}\boldsymbol{G}_{l-p^*}, \tag{31}$$

for $l > 0$, and $\boldsymbol{G}_l = \mathbf{O}$ for $l < 0$. At $h = 0$, the responses to an area-wide shock are GDP-weighted averages of the one shock generalized impulse responses, scaled by the standard deviation of the weighted arithmetic mean. Similarly to the standard GIRF, this leads to under- or overestimation of the total effect of these shocks. Therefore, this GDP-weighting approach differs from our multiple shock approach, where we analyze the simultaneous effect of one standard deviation shock in all countries' equity indices.

The traditional, generalized, and multiple shock forecast error variance decompositions can be derived in a manner analogous to Equations (8), (11) and (15). In these formulations, the matrices $\boldsymbol{B}^l$ are substituted with the matrix $\boldsymbol{G}_l$, leveraging the recursion in Equation (31).

4.1.1 Data

We use country-specific data for France, Germany, Spain and Italy. Each domestic model includes six variables, output, prices, short- and long-term government bond yields, stock prices and a stress index capturing uncertainty. Specifically, we consider output and prices as macroeconomic indicators. We use Chow-Lin interpolation to construct a monthly proxy for economic output for each country, where we use monthly industrial production as reference

series. Prices are modeled by the seasonally adjusted consumer price index (CPI). For financial variables, we use stock and bond market data. In particular, we use the 1 and 10 year government bond yields, the MSCI stock market index and the composite indicator of systematic stress (CISS), which measures the stress in financial markets for each of the four countries separately (Hollo et al., 2012). The consider six foreign-specific variables, capturing the relative spill-overs between countries, which are constructed as a trade-based weighted average of all the six domestic variables. We take the natural log of output, prices and stock prices.

The common model includes a monetary policy shock series as common monetary policy variable in Europe. The feedback variables in the common model are a GDP-weighted average of all the six domestic variables, capturing the general state of the Euro area economy as a whole.

4.1.2 Estimation

We estimate the model parameters in a country-per-country setting, as in Pesaran et al. (2004) and Burriel and Galesi (2018). We choose a parsimonious lag structure as in Burriel and Galesi (2018) based on information criteria; we set $p_i = 2$ for every country, such that we only consider contemporaneous relation to the exogenous variables, and we set both lags p_x, q_x to 2 for the common model.

We estimate the reduced-form parameters in a Bayesian fashion as this allows us to account for parameter uncertainty and to construct confidence bounds.[9] We use Gibbs sampling to draw from the joint posterior distribution of the reduced-form parameters, that is, we draw drawing from two conditional posterior distributions. In line with the Bayesian VAR literature, we choose a Minnesota type prior. Details on the exact procedure, prior choices and posterior distributions are reported in Appendix B. We report results based on a burn-in period of 5,000 draws, where we store every third of the following draws until we obtain 1,000 stable models from the joint posterior distribution. The Appendix reports the model diagnostics, where we show that the GVAR assumptions are adequately satisfied.

[9] Alternative methods are applying Bayesian shrinkage to the full model (Bańbura et al., 2010), or estimating the parameters with OLS in combination with a bootstrap procedure to construct confidence bounds (e.g., Dees et al., 2007; Burriel and Galesi, 2018).

By placing the shock series first in our model, we use it as an instrument for identifying a monetary policy shock. Plagborg-Møller and Wolf (2021) demonstrate that this approach yields valid impulse responses even for noninvertible shocks.

4.2 Identification

As Pesaran and Shin (1998) show, the GIRFs are equivalent to the orthogonal impulse response functions when the latter are prioritized in the ordering of the VAR. This implies that these shocks are pivotal in steering the system, given their instantaneous and widespread impact, with other variables reacting within the same time frame. By utilizing the GIRF and multiple shock impulse response functions, we inherently posit that the variables linked to the primary shocks are prioritized in the ordering, thereby leading the system's dynamics.

4.2.1 Monetary Policy and Financial Uncertainty

We focus on the effect of a monetary policy shock, triggering financial instability in vulnerable countries, on macroeconomic and financial variables. We use a measure based on the the market responses of short-term interest rates and the aggregate European stock index to an ECB monetary policy event as a proxy for a monetary policy shock, and country-specific stress indices as a proxy for uncertainty shocks. Monetary policy shocks can be captured through price changes in a tight window around a monetary policy announcement, as this captures the unexpected component of the announcement (see, e.g., Nakamura and Steinsson, 2018). When a central bank announcement start, financial markets have already priced in the central bank's systematic response to the state of the economy. Therefore, the interest rate surprise stemming from an ECB announcement can be interpreted as a measure for the causal effect of ECB's action. We consider the median monetary policy shock of Jarociński and Karadi (2020), who distinguish between two types of shocks—action and communication—based on the correlation to the surprise in interest rates and stock prices.[10] A monetary policy shock is characterized by negative correlation between the interest rate and stock

[10]The median ECB monetary policy shock is obtained from Marek Jarociński's website. The shock is based on the price change in 1, 3, 6 and 12 month interest rate swaps and stock prices in a 90 minute window around a ECB monetary policy event, obtained from the Euro Area Monetary Policy Event-Study Database of Altavilla et al. (2019).

price surprise. Monetary tightening leads to higher interest rates, increasing the discount rate. Further, stock prices decrease as the expected value of future dividends also decrease. The monetary policy shock therefore isolates the component of the ECB's action.

Examples of analyzing the effects of uncertainty shocks proxied by a volatility index in a VAR framework, are Bloom (2009, 2014), Bachmann et al. (2013), Gilchrist et al. (2014), Jurado et al. (2015) and Basu and Bundick (2017). They use a Cholesky decomposition to identify these uncertainty shocks. Ludvigson et al. (2021) highlight difficulty of identifying uncertainty shocks this way, as theory is unclear about the contemporaneous relations between uncertainty and, for example, real activity.The residual of the country-specific CISS represents a country-specific uncertainty shock. The CISS is a stress measure based on 15 realized volatility measures from mainly the money, equity, bond, and foreign exchange markets. We focus on uncertainty shocks in Italy and Spain.

For Cholesky identification, the ordering is crucial for identification. The literature also remains ambiguous about the ordering. For example, Leduc and Liu (2016) and Basu and Bundick (2017) assume that monetary policy contemporaneously respond to uncertainty by ordering the federal funds rate last, whereas Gertler and Karadi (2015) and Jarociński and Karadi (2020) assume that monetary policy affects all variables in the macro-financial VARs contemporaneously. Jurado et al. (2015) consider various ordering schemes, including uncertainty as last variable, and ordering uncertainty before the federal fund rate. Next to that, in the GVAR it is unclear what the ordering of variables should be in terms of what country comes first—making traditional impulse response analysis with contemporaneous zero restrictions less attractive (see, e.g., Pesaran et al., 2004; Dees et al., 2007). By ordering the common model first in orthogonalized IRF analysis, we assume that there is an exogenous monetary policy shock affecting all variables in the model contemporaneously. However, a shock in the systematic stress index only affects the variables ordered later than these variables. For example, when we consider the country order France, Germany, Italy, Spain, we assume that a shock in the Italian stress index only affects all the Spanish variables, including the real economic variables, contemporaneously, but this shock does not affect the French and German variables within the first month. Therefore, the anatomy of the GVAR framework makes it challenging to analyze country-specific shocks. The generalized

and multiple shock impulse response functions allow for contemporaneous responses between monetary policy and uncertainty, both ways, and infer identification of these relations by using the data. They therefore remain agnostic about the ordering of shocks occurring.

4.2.2 Area-wide Equity Shock

In absence of a very large economy in the model, it is not appropriate to analyze the impulse responses to, for example, a shock in a variable of an individual country as a proxy for an area-wide shock. In our model, a European stock market shock could be modeled as a shock in the German equity market, but this might not be appropriate as Germany is less than 50% of the Euro area GDP. The GVAR model enables us to assess the impact of area-wide shocks on countries separately. We illustrate this with a negative equity shock. We use the country-specific equity index residuals to proxy an Euro area-wide equity shock, capturing the aggregate Euro area component.

4.3 Results

Figure 3 shows the impulse response functions to a one standard deviation monetary policy shock, and one standard deviation uncertainty shocks for Italy and Spain. Each row corresponds to a country. The panels illustrate the median multiple impulse response functions for monetary policy and uncertainty shocks in the two Southern European countries, shown by the dark blue line. The shaded areas indicate the 16th/84th and 5th/95th percentile ranges of the posterior distribution. The dashed blue line corresponds to both traditional and generalized impulse response functions of a monetary policy shock, due to its primary ordering in the system. The summed traditional and generalized impulse response functions are denoted by the yellow and red lines, respectively.

The responses of the variables to a monetary tightening shock are consistent with standard economic theory. Real GDP and prices decrease, whereas government bond yields slightly increase (see Jarociński and Karadi, 2020). The amplified negative effect of an uncertainty shock on the real economy is in line with amongst others Bloom (2009), Leduc and Liu (2016) and Basu and Bundick (2017), who document declining real economic activity in

Figure 3: Impulse response functions to a monetary policy shock and simultaneous uncertainty shock in Italy and Spain

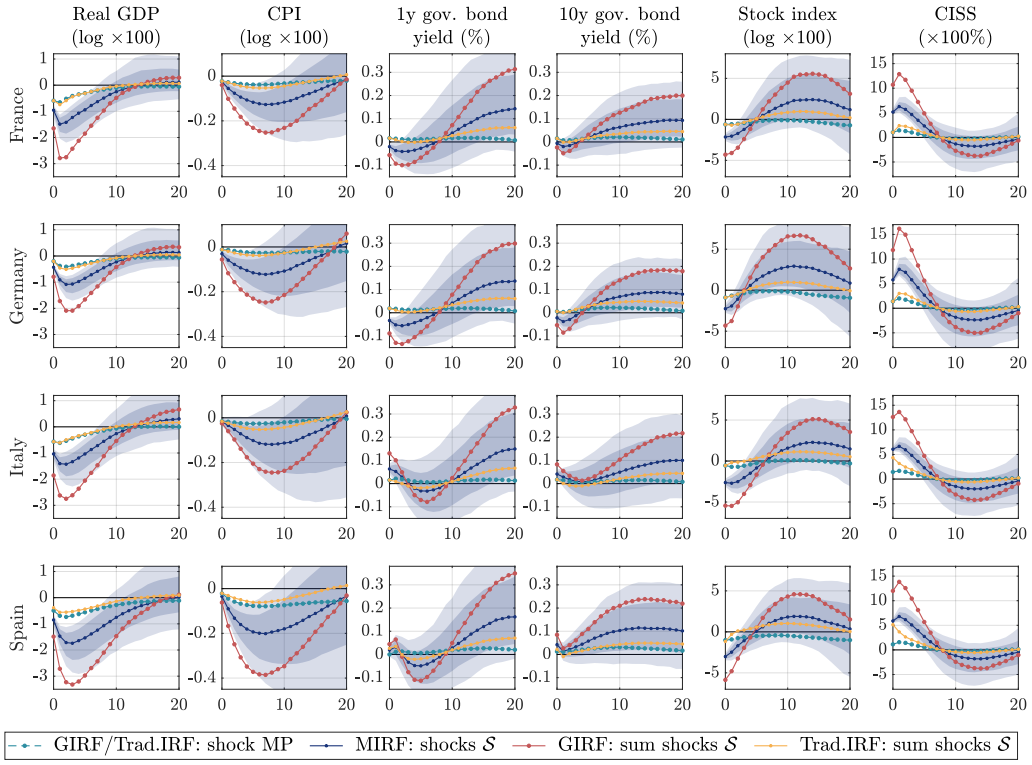

Note: All impulse responses correspond to the responses on a 20 month horizon. The solid dark blue lines correspond to the median multiple shock impulse response functions of a monetary policy shock combined with a shock in systematic risk in Italy and Spain. The darker (lighter) shaded areas correspond to 16–84th (5–95th) percentiles. The yellow lines correspond to the (coinciding) traditional and generalized median impulse responses to one monetary policy shock. The red and blue lines with correspond to the sum of the traditional and generalized median impulse response functions to all three shocks, respectively. The sample period is 01:1999-10:2022.

response to an uncertainty shock. In particular, the combined effect of a monetary policy shock and uncertainty shocks have a pronounced negative effect on real GDP and prices for all examined countries. This impact is most noticeable in Italy and Spain, although it is also apparent in France and Germany. While the immediate effects on short-term and long-term yields are minimal, a rise in these yields becomes evident over the span of one year. Further, stock prices across all countries decrease by roughly 2% within the first six months. It is worth noting that uncertainty shocks originating in Southern European nations can affect other countries in the Euro area—underlining the importance of clear and direct communication from the ECB to help avert such uncertainty.

The effect of a monetary policy shock on all variables is in general smaller in absolute terms compared to the joint effect of a monetary policy shock and uncertainty shocks. The sum of the traditional IRFs resemble the effect of the monetary policy shock, as for a lot of variables the initial response of the variables to an uncertainty shock is restricted to zero. The summed generalized IRFs overshoot the total effect. The highlight here is that for all concepts—single shock and summed versions of both traditional and generalized IRFs—the difference when compared to multiple shock impulse response functions is sizable, as they often fall outside the confidence bounds of the multiple shock IRFs, particularly within the first five months.

Table 3 shows the forecast error variance decompositions on impact and after 12 months for all methods. For the French real GDP, the generalized FEVD attributes 11.25% of the forecast error variance to a monetary policy shock, and 9.8% and 8.3% to uncertainty shocks in Italy and Spain, respectively. When considering the simultaneous effect of these shocks on the forecast error variance of the The simultaneous effect of these shocks on the forecast error variance of the French real GDP is 17.40%, in contrast to summing the three individual generalized FEVD (29.28%). This over-accounting becomes particularly evident in the stress indices of all countries, where the summed generalized FEVD exceeds 100%.

For all four stress indices, the generalized FEVD attributes approximately 5% of the forecast error variance to a monetary policy shock, both upon impact and after a year. This suggests that a monetary policy shock does not contribute much to the forecast error variance of the stress indices. The impulse responses further indicate that the stress indices exhibit minimal response to a monetary policy shock. In the case of real GDP and CPI, the forecast error variance either increases or remains consistent when comparing the immediate impact to the span of a year. However, for financial variables, there is a general decline in the forecast error variance when comparing the immediate impact to a year's duration.

Figure 4 shows the impulse response functions to a negative one standard deviation Euro area equity shock. Again, each row corresponds to a country, the panels illustrate the median impulse responses of negative shocks in the stock price indices of all four countries, and the shaded areas indicate 16th/84th and 5th/95th percentile ranges of the posterior distribution.

Table 3: Forecast Error Variance Decomposition of a monetary policy shock and simultaneous uncertainty shock in Italy and Spain

	France						Germany					
$h = 0$	Real GDP	CPI	1y g. yield	10y g. yield	Stock index	CISS	Real GDP	CPI	1y g. yield	10y g. yield	Stock index	CISS
$\gamma^g_{i,1}(h)$	11.25	1.54	0.61	0.51	1.26	3.13	3.58	0.21	0.96	0.09	2.00	4.26
$\gamma^g_{i,2}(h)$	9.80	0.56	2.59	0.52	11.89	68.27	7.38	0.52	7.54	1.79	7.83	62.60
$\gamma^g_{i,3}(h)$	8.27	0.10	3.70	1.17	10.39	67.19	8.44	0.89	8.13	2.34	6.78	55.43
$\gamma^{\mathcal{S}}_i(h)$	17.40	2.31	5.26	2.23	12.51	73.69	10.61	1.05	11.38	2.80	8.77	64.79
Sum $\gamma^g_{i,j}(h)$	29.28	2.22	7.03	2.31	23.66	138.58	19.55	1.65	16.58	4.27	16.56	122.15
Sum $\gamma^t_{i,j}(h)$	11.25	1.54	0.61	0.51	1.26	3.13	3.58	0.21	0.96	0.09	2.00	4.26
$h = 12$												
$\gamma^g_{i,1}(h)$	11.48	1.84	0.48	0.43	1.09	3.52	6.95	0.32	0.69	0.20	1.34	4.27
$\gamma^g_{i,2}(h)$	24.51	5.10	3.87	1.24	9.65	64.99	25.43	3.08	8.32	2.79	6.25	60.65
$\gamma^g_{i,3}(h)$	22.48	3.90	4.72	1.83	8.27	61.78	25.21	3.74	8.73	3.39	5.56	54.16
$\gamma^{\mathcal{S}}_i(h)$	31.53	6.30	6.20	2.75	10.14	69.19	30.06	3.99	11.57	4.09	7.09	63.11
Sum $\gamma^g_{i,j}(h)$	58.56	10.87	9.20	3.63	18.89	130.46	57.67	7.19	17.80	6.45	13.23	119.04
Sum $\gamma^t_{i,j}(h)$	11.56	1.88	0.55	0.49	1.13	4.10	7.20	0.36	0.75	0.26	1.43	4.75
	Italy						Spain					
$h = 0$	Real GDP	CPI	1y g. yield	10y g. yield	Stock index	CISS	Real GDP	CPI	1y g. yield	10y g. yield	Stock index	CISS
$\gamma^g_{i,1}(h)$	9.31	0.46	0.19	0.37	0.84	5.69	8.14	0.47	0.02	0.23	2.73	3.64
$\gamma^g_{i,2}(h)$	13.19	0.07	3.26	2.21	18.47	100.00	8.16	0.52	0.69	2.16	14.97	70.61
$\gamma^g_{i,3}(h)$	11.04	0.18	2.27	0.82	14.70	70.61	8.45	0.33	0.25	1.50	16.55	100.00
$\gamma^{\mathcal{S}}_i(h)$	18.66	1.13	3.31	2.79	18.74	100.00	14.33	0.87	1.00	2.27	17.92	100.00
Sum $\gamma^g_{i,j}(h)$	33.68	0.78	5.75	3.43	33.95	176.29	24.79	1.38	0.99	3.94	34.35	174.34
Sum $\gamma^t_{i,j}(h)$	9.31	0.46	0.19	0.37	0.84	28.58	8.55	0.50	0.68	0.36	2.82	29.73
$h = 12$												
$\gamma^g_{i,1}(h)$	9.56	0.53	0.30	0.32	1.00	5.08	9.63	1.49	0.13	0.31	2.28	4.12
$\gamma^g_{i,2}(h)$	23.46	1.48	2.70	1.77	14.98	79.27	22.00	4.42	1.35	1.82	11.23	68.06
$\gamma^g_{i,3}(h)$	22.32	1.91	2.11	0.88	13.00	61.79	19.88	3.51	1.07	1.32	11.40	80.81
$\gamma^{\mathcal{S}}_i(h)$	29.35	2.58	2.94	2.30	15.71	80.49	27.57	5.14	1.89	2.38	13.33	84.29
Sum $\gamma^g_{i,j}(h)$	55.25	3.89	5.14	2.98	29.10	146.14	51.49	9.35	2.65	3.50	24.97	153.12
Sum $\gamma^t_{i,j}(h)$	9.66	0.68	0.56	0.53	1.78	16.38	10.08	1.63	0.73	0.65	2.88	17.13

Note: Median Forecast Error Variance Decomposition (FEVD) in percentages, upon impact ($h = 0$) and after one year ($h = 12$). Generalized $\left(\gamma^g_{i,j}(h)\right)$ for every shock $j \in \mathcal{S}$, multiple shock $\left(\gamma^{\mathcal{S}}_i(h)\right)$, and summed generalized and tradidional FEVD, for variable i for each country. The sample period is 01:1999-10:2022.

Figure 4: Impulse response functions to a negative area-wide equity shock

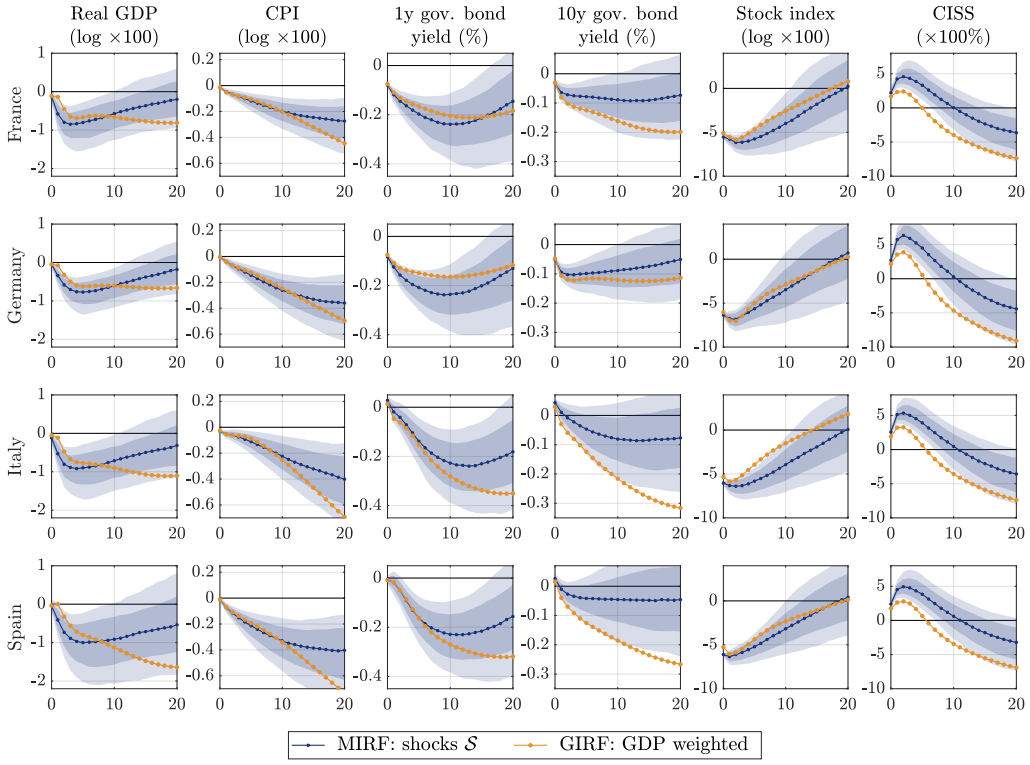

Note: All impulse responses correspond to the responses on a 20 month horizon. The solid dark blue lines correspond to the median multiple shock impulse response functions of an equity shock in all countries. The darker (lighter) shaded areas correspond to 16–84th (5–95th) percentiles. The orange lines correspond to generalized GDP-weighted median impulse responses to all four country-specific equity shocks. The sample period is 01:1999-10:2022.

The orange line corresponds to the GDP-weighted generalized impulse responses, as defined in the literature. In general, the macroeconomic effects are very similar across all four countries. The 1-year government bond yields of Italy and Spain show no initial reaction, but the impact becomes evident after approximately 3 months. The short end of the yield curve is more affected than the long end. Consistent with Baele et al. (2004), who documented a rise in financial integration within the Euro area from 1973 to 2003, we observe that local stock return indices exhibit a similar response to an area-wide equity shock, indicating a deepening equity market integration in the Euro zone over the period from 1999 until 2022.

The figure shows that for especially after one year, the impulse responses of the multiple shocks and the GDP-weighted area-wide shock differ. The GDP-weighted impulse response functions tend to diverge—especially on longer horizons. Internet Appendix shows

the responses over a 6 year horizon. The multiple shock impulse responses provide a more historically consistent transmission of an area-wide equity shock, as the responses diminish over a longer horizon.

5 Conclusion

This paper introduces multiple shock impulse response functions, a novel method that facilitates the examination of the cumulative effects of simultaneous model shocks within a single period of time. By taking into account the dependence between shocks, they provide a comprehensive framework to understand the total impact of simultaneous shocks on a system. This concept is versatile, suitable for a broad range of multivariate time series models, and serves as a generalization of the individual generalized impulse response functions. This tool proves particularly useful in scenarios where the simultaneous impact of model shocks represents an underlying primitive structural shock. Additionally, it adeptly uses region-specific model shocks as effective proxies for a singular, overarching global structural shock.

The properties of multiple shock impulse response functions are examined within the context of a first order vector autoregression model with normally distributed error terms. The closed-form solutions of traditional and general impulse response functions of Sims (1980) and Koop et al. (1996) are revisited, and we derive a closed-form solution for the multiple shock impulse response functions. We discuss their relation to each other, and show using simulations that multiple shock impulse response functions are necessary in order to accurately analyze the total effect of multiple shocks, as summing individual impulse responses leads to over- or underestimation depending on the correlation between the shocks. We further show in a mixed-frequency simulation setting that multiple impulse response functions are useful to address potential temporal aggregation issues, as these might arise when multiple shocks occur concurrently within a single period of the observed data frequency. The multiple shock impulse response functions closely replicate the true underlying structural dynamics, offering a more refined portrayal of combined high-frequency structural behaviors, especially in contrast to merely aggregating individual low-frequency impulse responses.

We apply multiple shock impulse response functions in a global vector autoregression

framework of Pesaran et al. (2004), and focus on four European countries: France, Germany, Italy, and Spain. The multiple shock approach proves beneficial in this setting, particularly when addressing issues arising from numerous shocks within a single month. Additionally, it does not require assumptions on the ordering of variables. This is crucial, given that events unfold at a quicker pace than our monthly model measures, combined with the undetermined hierarchy of countries in the model.

We focus on two types of shocks. First, we study monetary policy and uncertainty. The combined effect of monetary policy and uncertainty shocks is particularly evident in how a monetary policy shock can trigger financial uncertainty, reshaping the understanding of systematic risk. This was prominently observed during the European debt crisis when the European Central Bank's decision to increase interest rates heightened financial uncertainty in lower credit rating EMU countries. These shifts usually happen within a month, highlighting the need for a way to understand the effects of many shocks happening at once in this short period. We proxy this by using the multiple shock approach on the interaction between monetary policy and uncertainty shocks stemming from Italy and Spain. For the orthogonalized, generalized and multiple shock impulse response concepts, we find responses consistent with economic theory. The interaction between monetary policy and uncertainty shocks amplifies the effects on economic and financial variables, especially real GDP, with effects nearly doubling when these shocks coincide. Such uncertainties also influence major economies like France and Germany. The multiple shock impulse response functions emerge as a valuable tool for stress testing and assessing economic robustness. Clear communication from the ECB can help mitigate these effects. Second, we focus on an area-wide negative equity shock. When analyzing area-wide negative equity shocks, the multiple shock method aligns more closely with theoretical expectations over the long-term, compared to the GDP-weighted average of country-specific shocks, which tends to deviate over time. This highlights the ability of the multiple shock method in capturing long-term trends that align with theoretical expectations.

In conclusion, this study makes a contribution to impulse response analysis by introducing multiple shock impulse response functions, providing a practical and effective tool to navigate the challenges associated with simultaneous shocks in multivariate models. It provides an

alternative way of looking at the complex interconnected nature of economic and financial systems. For further research, it would be interesting to explore non-linear dynamics, such as second order dynamics, through the lens of multiple shock impulse response functions.

References

Altavilla, C., L. Brugnolini, R. S. Gürkaynak, R. Motto, and G. Ragusa (2019). Measuring euro area monetary policy. *Journal of Monetary Economics 108*, 162–179.

Bachmann, R., S. Elstner, and E. R. Sims (2013). Uncertainty and economic activity: Evidence from business survey data. *American Economic Journal: Macroeconomics 5*(2), 217–249.

Baele, L., A. Ferrando, P. Hördahl, E. Krylova, and C. Monnet (2004). Measuring financial integration in the euro area.

Bańbura, M., D. Giannone, and L. Reichlin (2010). Large bayesian vector auto regressions. *Journal of Applied Econometrics 25*(1), 71–92.

Basu, S. and B. Bundick (2017). Uncertainty shocks in a model of effective demand. *Econometrica 85*(3), 937–958.

Beirne, J. and M. Fratzscher (2013). The pricing of sovereign risk and contagion during the european sovereign debt crisis. *Journal of International Money and Finance 34*, 60–82.

Billio, M., M. Getmansky, A. W. Lo, and L. Pelizzon (2012). Econometric measures of connectedness and systemic risk in the finance and insurance sectors. *Journal of Financial Economics 104*(3), 535–559.

Blanchard, O. J. and D. Quah (1989). The dynamic effects of aggregate demand and supply disturbances. *American Economic Review 79*(4), 655–673.

Bloom, N. (2009). The impact of uncertainty shocks. *Econometrica 77*(3), 623–685.

Bloom, N. (2014). Fluctuations in uncertainty. *Journal of Economic Perspectives 28*(2), 153–176.

Burriel, P. and A. Galesi (2018). Uncovering the heterogeneous effects of ECB unconventional monetary policies across euro area countries. *European Economic Review 101*, 210–229.

Christiano, L. J., M. Eichenbaum, and C. L. Evans (1999). Monetary policy shocks: What have we learned and to what end? In M. Woodford and J. Taylor (Eds.), *Handbook of Macroeconomics*, Volume 1, pp. 65–148. Elsevier, Amsterdam.

Dees, S., F. d. Mauro, M. H. Pesaran, and L. V. Smith (2007). Exploring the international linkages of the euro area: a global VAR analysis. *Journal of Applied Econometrics 22*(1), 1–38.

Dickey, D. A. and W. A. Fuller (1979). Distribution of the estimators for autoregressive time series with a unit root. *Journal of the American Statistical Association 74*(366a), 427–431.

Fernández-Villaverde, J., J. F. Rubio-Ramírez, T. J. Sargent, and M. W. Watson (2007). ABCs (and Ds) of understanding VARs. *American Economic Review 97*(3), 1021–1026.

Gali, J. (1999). Technology, employment, and the business cycle: do technology shocks explain aggregate fluctuations? *American Economic Review 89*(1), 249–271.

Gertler, M. and P. Karadi (2015). Monetary policy surprises, credit costs, and economic activity. *American Economic Journal: Macroeconomics 7*(1), 44–76.

Ghysels, E. (2016). Macroeconomics and the reality of mixed frequency data. *Journal of Econometrics 193*(2), 294–314.

Ghysels, E., P. Santa-Clara, and R. Valkanov (2004). The midas touch: Mixed data sampling regression models. Working Paper.

Ghysels, E., A. Sinko, and R. Valkanov (2007). Midas regressions: Further results and new directions. *Econometric Reviews 26*(1), 53–90.

Gilchrist, S., J. W. Sim, and E. Zakrajšek (2014). Uncertainty, financial frictions, and investment dynamics. NBER Working Paper No. 20038.

Hollo, D., M. Kremer, and M. Lo Duca (2012). CISS–a composite indicator of systemic stress in the financial system. ECB Working Paper, No. 1426.

Hubrich, K. and R. J. Tetlow (2015). Financial stress and economic dynamics: The transmission of crises. *Journal of Monetary Economics 70*, 100–115.

Jarociński, M. and P. Karadi (2020). Deconstructing monetary policy surprises–the role of information shocks. *American Economic Journal: Macroeconomics 12*(2), 1–43.

Jurado, K., S. C. Ludvigson, and S. Ng (2015). Measuring uncertainty. *American Economic Review 105*(3), 1177–1216.

Koop, G., M. H. Pesaran, and S. M. Potter (1996). Impulse response analysis in nonlinear multivariate models. *Journal of Econometrics 74*(1), 119–147.

Lane, P. R. (2012). The european sovereign debt crisis. *Journal of Economic Perspectives 26*(3), 49–68.

Leduc, S. and Z. Liu (2016). Uncertainty shocks are aggregate demand shocks. *Journal of Monetary Economics 82*, 20–35.

Litterman, R. B. (1986). Forecasting with bayesian vector autoregressions—five years of experience. *Journal of Business & Economic Statistics 4*(1), 25–38.

Ludvigson, S. C., S. Ma, and S. Ng (2021). Uncertainty and business cycles: exogenous impulse or endogenous response? *American Economic Journal: Macroeconomics 13*(4), 369–410.

Lütkepohl, H. (2005). *New introduction to multiple time series analysis*. Springer Science & Business Media.

Nakamura, E. and J. Steinsson (2018). High-frequency identification of monetary non-neutrality: the information effect. *The Quarterly Journal of Economics 133*(3), 1283–1330.

Pesaran, H. H. and Y. Shin (1998). Generalized impulse response analysis in linear multivariate models. *Economics Letters 58*(1), 17–29.

Pesaran, M. H., T. Schuermann, and S. M. Weiner (2004). Modeling regional interdependencies using a global error-correcting macroeconometric model. *Journal of Business & Economic Statistics 22*(2), 129–162.

Plagborg-Møller, M. and C. K. Wolf (2021). Local projections and vars estimate the same impulse responses. *Econometrica 89*(2), 955–980.

Rambachan, A. and N. Shephard (2021). When do common time series estimands have nonparametric causal meaning? Working paper.

Ramey, V. A. (2016). *Macroeconomic shocks and their propagation*, Volume 2. Elsevier.

Rostagno, M., C. Altavilla, G. Carboni, W. Lemke, R. Motto, A. S. Guilhem, and J. Yiangou (2019). A tale of two decades: the ECB's monetary policy at 20.

Sims, C. A. (1972). Money, income, and causality. *American Economic Review 62*(4), 540–552.

Sims, C. A. (1980). Macroeconomics and reality. *Econometrica 48*(1), 1–48.

Uhlig, H. (2005). What are the effects of monetary policy on output? results from an agnostic identification procedure. *Journal of Monetary Economics 52*(2), 381–419.

Supplementary Material to:

"Multiple Shock Impulse Response Functions"

A Derivations Linear Vector Autoregression Model

Derivation of the VMA of Equation (6) of the VAR Process

The VMA representation of the linear VAR(1) model is

$$\begin{aligned}
\boldsymbol{y}_t &= \boldsymbol{b} + \boldsymbol{B}\boldsymbol{y}_{t-1} + \boldsymbol{u}_t, \\
&= \boldsymbol{b} + \boldsymbol{B}(\boldsymbol{b} + \boldsymbol{B}\boldsymbol{y}_{t-2} + \boldsymbol{u}_{t-1}) + \boldsymbol{u}_t, \\
&= (\boldsymbol{I}_n + \boldsymbol{B})\boldsymbol{b} + \boldsymbol{B}^2\boldsymbol{y}_{t-2} + \boldsymbol{B}\boldsymbol{u}_{t-1} + \boldsymbol{u}_t, \\
&= ... \\
&= (\boldsymbol{I}_n + \boldsymbol{B} + ... + \boldsymbol{B}^{j-1})\boldsymbol{b} + \boldsymbol{B}^j\boldsymbol{y}_{t-j} + \sum_{i=0}^{j-1}\boldsymbol{B}^i\boldsymbol{u}_{t-i},
\end{aligned}$$

by recursively substituting the VAR equation. Under Assumption 2, it holds that the sequence $\boldsymbol{B}^i$ is absolutely square summable and therefore the infinite sum of $\sum_{i=0}^{j-1}\boldsymbol{B}^i\boldsymbol{u}_{t-i}$ exists in mean square. As $j \longrightarrow \infty$, it holds that $\boldsymbol{B}^j \to \mathbf{O}$ and $(\boldsymbol{I}_n + \boldsymbol{B} + ... + \boldsymbol{B}^{j-1})\boldsymbol{b} \longrightarrow (\boldsymbol{I}_n - \boldsymbol{B})^{-1}\boldsymbol{b}$, according to a standard geometric series. Thus, when $j \longrightarrow \infty$

$$\begin{aligned}
\boldsymbol{y}_t &= (\boldsymbol{I}_n - \boldsymbol{B})^{-1}\boldsymbol{b} + \sum_{j=0}^{\infty}\boldsymbol{B}^j\boldsymbol{u}_{t-j}, \\
&= \boldsymbol{\mu} + \sum_{j=0}^{\infty}\boldsymbol{B}^j\boldsymbol{u}_{t-j}. \qquad \text{(A.1)}
\end{aligned}$$

Derivation of the Impulse Response Functions

The traditional impulse response functions for a linear vector autoregression can be derived from taking the expectations of the shifted VMA representation of Equation (6) and the structural relation $\boldsymbol{\varepsilon}_t = \boldsymbol{C}\boldsymbol{u}_t$. The VMA for $\boldsymbol{y}_{t+h}$ denotes

$$\begin{aligned}
\boldsymbol{y}_{t+h} &= \boldsymbol{\mu} + \sum_{j=0}^{\infty}\boldsymbol{B}^j\boldsymbol{C}\boldsymbol{\varepsilon}_{t+h-j} \\
&= \boldsymbol{\mu} + \boldsymbol{C}\boldsymbol{\varepsilon}_{t+h} + \boldsymbol{B}\boldsymbol{C}\boldsymbol{\varepsilon}_{t+h-1} + \boldsymbol{B}^2\boldsymbol{C}\boldsymbol{\varepsilon}_{t+h-2} + ... + \boldsymbol{B}^h\boldsymbol{C}\boldsymbol{\varepsilon}_t + \boldsymbol{B}^{h+1}\boldsymbol{C}\boldsymbol{\varepsilon}_{t-1} + ...
\end{aligned}$$

Inserting the expression in both conditional expectations, this results in the perturbed path

$$\begin{aligned}
&\mathbb{E}[\boldsymbol{y}_{t+h} \mid \varepsilon_{s,t} = \delta_s, \varepsilon_{j,t} = 0 \, \forall j \neq s, \boldsymbol{\varepsilon}_{t+1} = ... = \boldsymbol{\varepsilon}_{t+h} = \boldsymbol{0}, \boldsymbol{\omega}_t] \\
&\quad = \boldsymbol{\mu} + \mathbb{E}[\boldsymbol{C}\boldsymbol{\varepsilon}_t \mid \varepsilon_{s,t} = \delta_s, \varepsilon_{j,t} = 0 \, \forall j \neq s, \boldsymbol{\varepsilon}_{t+1} = ... = \boldsymbol{\varepsilon}_{t+h} = \boldsymbol{0}, \boldsymbol{\omega}_t] + \boldsymbol{B}^{h+1}\boldsymbol{C}\boldsymbol{\varepsilon}_{t-1} + ... \\
&\quad = \boldsymbol{\mu} + \boldsymbol{C}\boldsymbol{e}_s\delta_s + \boldsymbol{B}^{h+1}\boldsymbol{C}\boldsymbol{\varepsilon}_{t-1} + ...
\end{aligned}$$

and the benchmark

$$\begin{aligned}
&\mathbb{E}[\boldsymbol{y}_{t+h} \mid \boldsymbol{\varepsilon}_t = \boldsymbol{\varepsilon}_{t+1} = ... = \boldsymbol{\varepsilon}_{t+h} = \boldsymbol{0}, \boldsymbol{\omega}_t] \\
&\quad = \boldsymbol{\mu} + \mathbb{E}[\boldsymbol{C}\boldsymbol{\varepsilon}_t \mid \boldsymbol{\varepsilon}_t = \boldsymbol{\varepsilon}_{t+1} = ... = \boldsymbol{\varepsilon}_{t+h} = \boldsymbol{0}, \boldsymbol{\omega}_t] + \boldsymbol{B}^{h+1}\boldsymbol{C}\boldsymbol{\varepsilon}_{t-1} + ... \\
&\quad = \boldsymbol{\mu} + \boldsymbol{B}^{h+1}\boldsymbol{C}\boldsymbol{\varepsilon}_{t-1} + ...
\end{aligned}$$

Thus, the difference is defined as $\boldsymbol{\Psi}^t(h, \boldsymbol{\varepsilon}_t = \delta_s, \boldsymbol{\omega}_{t-1}) = \boldsymbol{C}\boldsymbol{e}_s\delta_s$, where $\boldsymbol{e}_s$ denotes the selection vector.

In order to derive the generalized impulse response functions for a linear VAR(1) model, we split the infinite sum of the VMA as

$$\boldsymbol{y}_{t+h} = \boldsymbol{\mu} + \boldsymbol{u}_{t+h} + \boldsymbol{B}\boldsymbol{u}_{t+h-1} + ... + \boldsymbol{B}^h\boldsymbol{u}_t + \sum_{j=1}^{\infty} \boldsymbol{B}^{h+j}\boldsymbol{u}_{t-j}. \tag{A.2}$$

Next to that, as we assume normality of the residuals, we use the properties of the conditional expectations of the multivariate normal distribution in order to obtain the following expression for the expectations

$$\mathbb{E}[\boldsymbol{y}_{t+h} \mid u_{s,t} = \delta_s, \mathcal{I}_{t-1}] = \boldsymbol{\mu} + \boldsymbol{B}^h\boldsymbol{\Sigma}\boldsymbol{e}_s(\sigma_{ss})^{-1}\delta_s + \sum_{j=1}^{\infty} \boldsymbol{B}^{h+j}\boldsymbol{u}_{t-j}, \tag{A.3}$$

and

$$\mathbb{E}[\boldsymbol{y}_{t+h} \mid \mathcal{I}_{t-1}] = \boldsymbol{\mu} + \sum_{j=1}^{\infty} \boldsymbol{B}^{h+j}\boldsymbol{u}_{t-j}. \tag{A.4}$$

Again, $\boldsymbol{e}_s$ denotes the selection vector and σ_{ss} denotes the variance of shock s, i.e., the (s, s)-th entry of the covariance matrix $\boldsymbol{\Sigma}$.

For the multiple shock impulse response functions, the first conditional expectation is

then

$$\mathbb{E}[\boldsymbol{y}_{t+h} \mid \boldsymbol{u}_{\mathcal{S},t} = \boldsymbol{\delta}_{\mathcal{S}}, \mathcal{I}_{t-1}] = \boldsymbol{\mu} + \boldsymbol{B}^h \mathbb{E}[\boldsymbol{u}_t \mid \boldsymbol{u}_{\mathcal{S},t} = \boldsymbol{\delta}_{\mathcal{S}}, \mathcal{I}_{t-1}] + \sum_{j=1}^{\infty} \boldsymbol{B}^{h+j} \boldsymbol{u}_{t-j}$$
$$= \boldsymbol{\mu} + \boldsymbol{B}^h \boldsymbol{\Sigma} \boldsymbol{P} (\boldsymbol{P}' \boldsymbol{\Sigma} \boldsymbol{P})^{-1} \boldsymbol{\delta}_{\mathcal{S}} + \sum_{j=1}^{\infty} \boldsymbol{B}^{h+j} \boldsymbol{u}_{t-j}, \tag{A.5}$$

where $\boldsymbol{P}$ denotes an $n \times m$ permutation matrix, containing m selection vectors where the selection indices correspond to the indices $\mathcal{S}$ of interest. The multiple shock impulse response functions are then defined as the difference between Equation (A.5) and the benchmark given by Equation (A.4).

Forecast Error Variance Decomposition of the VAR Process

We derive the variance of the forecast error using the VMA in Equation (A.1). The forecast error at horizon h, $\boldsymbol{\Delta}_{t+h}$, denotes

$$\boldsymbol{\Delta}_{t+h} = \sum_{l=0}^{h} \boldsymbol{B}^l \boldsymbol{u}_{t+h-l}. \tag{A.6}$$

Then, $\text{var}(\boldsymbol{\Delta}_{t+h}) = \sum_{l=0}^{h} \boldsymbol{B}^l (\boldsymbol{B}^l)'$, using the fact that $\text{var}(\boldsymbol{u}_t) = \boldsymbol{\Sigma}$ for all t. We then define the improvement of knowing the forecast error if shock s is known for the traditional orthogonal error

$$\boldsymbol{\Delta}^t_{t+h,s} = \sum_{l=0}^{h} \boldsymbol{B}^l \Big(\boldsymbol{u}_{t+h-l} - \boldsymbol{e}_s u_{s,t+h-l} \Big). \tag{A.7}$$

The variance is then $\text{var}(\boldsymbol{\Delta}^t_{t+h,s}) = \sum_{l=0}^{h} \boldsymbol{B}^l (\boldsymbol{B}^l)' - \sum_{l=0}^{h} \boldsymbol{B}^l \boldsymbol{e}_s \boldsymbol{e}_s' (\boldsymbol{B}^l)'$. The forecast error variance decomposition for variable i of shock s is then

$$\gamma^t_{i,s}(h) = \frac{\boldsymbol{e}_s' \Big(\text{var}(\boldsymbol{\Delta}_{t+h}) - \text{var}(\boldsymbol{\Delta}^t_{t+h,s}) \Big) \boldsymbol{e}_s}{\boldsymbol{e}_s' \Big(\text{var}(\boldsymbol{\Delta}_{t+h}) \Big) \boldsymbol{e}_s}. \tag{A.8}$$

For the generalized forecast error, conditional on shock s, is

$$\boldsymbol{\Delta}^g_{t+h,s} = \sum_{l=0}^{h} \boldsymbol{B}^l \Big(\boldsymbol{u}_{t+h-l} - \mathbb{E}[u_{s,t+h-l} | ...] \Big) \tag{A.9}$$
$$= \sum_{l=0}^{h} \boldsymbol{B}^l \Big(\boldsymbol{u}_{t+h-l} - (\sigma_{ss})^{-1} \boldsymbol{\Sigma} \boldsymbol{e}_s u_{s,t+h-l} \Big). \tag{A.10}$$

The corresponding variance is $\text{var}(\boldsymbol{\Delta}^g_{t+h,s}) = \sum_{l=0}^{h} \boldsymbol{B}^l(\boldsymbol{B}^l)' - (\sigma_{ss})^{-1} \sum_{l=0}^{h} \boldsymbol{B}^l \boldsymbol{\Sigma} \boldsymbol{e}_s \boldsymbol{e}_s' \boldsymbol{\Sigma} (\boldsymbol{B}^l)'$. The corresponding FEVD is then $\gamma^g_{i,s}(h)$, as in Equation (A.7).

B Application Global Vector Autoregression

Derivation of the Global Vector Autoregression (GVAR) Model

Let $\boldsymbol{y}_t$ denote a $k \times 1$ vector containing all stacked domestic variables, where $k = \sum_{i=1}^{N} k_i$, such that $\boldsymbol{y}_t = \left[\boldsymbol{y}_{1,t}', ..., \boldsymbol{y}_{N,t}'\right]'$. We rewrite each domestic model of Equation (23) for country $i = 1, ..., N$ in terms of $\boldsymbol{y}_t$ as

$$\underbrace{\begin{bmatrix}\boldsymbol{I}_{k_i} & -\boldsymbol{\Lambda}_{i,0}\end{bmatrix}\boldsymbol{W}_i}_{\boldsymbol{G}_{i,0}}\boldsymbol{y}_t = \boldsymbol{c}_i + \sum_{\ell=1}^{p_i}\underbrace{\begin{bmatrix}\boldsymbol{C}_{i,\ell} & \boldsymbol{\Lambda}_{i,\ell}\end{bmatrix}\boldsymbol{W}_i}_{\boldsymbol{G}_{i,j}}\boldsymbol{y}_{t-\ell} + \sum_{\ell=0}^{q_i}\boldsymbol{\Gamma}_{i,\ell}\boldsymbol{x}_{t-\ell} + \boldsymbol{\eta}_{i,t}, \tag{A.11}$$

by splitting the sum of the country-specific exogenous variables $\boldsymbol{y}^*_{i,t}$ into a contemporaneous part and historical parts, and using Equation (24). The $(k_i + k_i^*) \times k$ country-specific weight matrix $\boldsymbol{W}_i$ contains the elements $w_{i,j}$. The first k_i rows of $\boldsymbol{W}_i$ correspond to the domestic variables itself, and the remaining k_i^* rows correspond to the selected weighted foreign variables. We stack the N domestic VAR models of Equation (A.11) as

$$\begin{bmatrix}\boldsymbol{G}_{1,0}\\ \boldsymbol{G}_{2,0}\\ \vdots\\ \boldsymbol{G}_{N,0}\end{bmatrix}\begin{bmatrix}\boldsymbol{y}_{1,t}\\ \boldsymbol{y}_{2,t}\\ \vdots\\ \boldsymbol{y}_{N,t}\end{bmatrix} = \begin{bmatrix}\boldsymbol{c}_1\\ \boldsymbol{c}_2\\ \vdots\\ \boldsymbol{c}_N\end{bmatrix} + \sum_{\ell=1}^{\max(p,q)}\begin{bmatrix}\boldsymbol{G}_{1,\ell}\\ \boldsymbol{G}_{2,\ell}\\ \vdots\\ \boldsymbol{G}_{N,\ell}\end{bmatrix}\begin{bmatrix}\boldsymbol{y}_{1,t-\ell}\\ \boldsymbol{y}_{2,t-\ell}\\ \vdots\\ \boldsymbol{y}_{N,t-\ell}\end{bmatrix} + \sum_{\ell=0}^{q}\begin{bmatrix}\boldsymbol{\Gamma}_{1,\ell}\\ \boldsymbol{\Gamma}_{2,\ell}\\ \vdots\\ \boldsymbol{\Gamma}_{N,\ell}\end{bmatrix}\boldsymbol{x}_{t-\ell} + \begin{bmatrix}\boldsymbol{\eta}_{1,t}\\ \boldsymbol{\eta}_{2,t}\\ \vdots\\ \boldsymbol{\eta}_{N,t}\end{bmatrix}, \tag{A.12}$$

or as

$$\boldsymbol{G}_0\boldsymbol{y}_t = \boldsymbol{c} + \sum_{\ell=1}^{\max(p,q)}\boldsymbol{G}_\ell\boldsymbol{y}_{t-\ell} + \sum_{\ell=0}^{q}\boldsymbol{\Gamma}_\ell\boldsymbol{x}_{t-\ell} + \boldsymbol{\eta}_t, \tag{A.13}$$

with $p = \max_i(p_i)$ and $q = \max_i(q_i)$. We rearrange Equation (A.13) as

$$-\boldsymbol{\Gamma}_0\boldsymbol{x}_t + \boldsymbol{G}_0\boldsymbol{y}_t = \boldsymbol{c} + \sum_{\ell=1}^{q}\boldsymbol{\Gamma}_\ell\boldsymbol{x}_{t-\ell} + \sum_{\ell=1}^{\max(p,q)}\boldsymbol{G}_\ell\boldsymbol{y}_{t-\ell} + \boldsymbol{\eta}_t. \tag{A.14}$$

We then rewrite the common variable equation Equation (25) as

$$\boldsymbol{x}_t - \boldsymbol{\Phi}_0\widetilde{\boldsymbol{W}}\boldsymbol{y}_t = \boldsymbol{c}_x + \sum_{\ell=1}^{p_x}\boldsymbol{\Theta}_\ell\boldsymbol{x}_{t-\ell} + \sum_{\ell=1}^{q_x}\boldsymbol{\Phi}_\ell\widetilde{\boldsymbol{W}}\boldsymbol{y}_{t-\ell} + \boldsymbol{\eta}_{x,t}. \tag{A.15}$$

Both Equation (A.14) and Equation (A.15) have a similar structure. We then stack the common variable model on the N domestic models and obtain

$$\underbrace{\begin{bmatrix} \boldsymbol{I} & -\boldsymbol{\Phi}_0\widetilde{\boldsymbol{W}} \\ -\boldsymbol{\Gamma}_0 & \boldsymbol{G}_0 \end{bmatrix}}_{\boldsymbol{H}_0} \begin{bmatrix} \boldsymbol{x}_t \\ \boldsymbol{y}_t \end{bmatrix} = \begin{bmatrix} \boldsymbol{c}_x \\ \boldsymbol{c} \end{bmatrix} + \sum_{\ell=1}^{\max(p,q,q_x)} \underbrace{\begin{bmatrix} \boldsymbol{\Theta}_\ell & \boldsymbol{\Phi}_\ell\widetilde{\boldsymbol{W}} \\ \boldsymbol{\Gamma}_\ell & \boldsymbol{G}_\ell \end{bmatrix}}_{\boldsymbol{H}_\ell} \begin{bmatrix} \boldsymbol{x}_{t-\ell} \\ \boldsymbol{y}_{t-\ell} \end{bmatrix} + \begin{bmatrix} \boldsymbol{\eta}_{x,t} \\ \boldsymbol{\eta}_t \end{bmatrix}, \tag{A.16}$$

or

$$\boldsymbol{H}_0\boldsymbol{z}_t = \boldsymbol{h}_0 + \sum_{\ell=1}^{\max(p,q,q_x)} \boldsymbol{H}_\ell\boldsymbol{z}_{t-\ell} + \boldsymbol{\varepsilon}_t, \tag{A.17}$$

where $\boldsymbol{z}_t = [\boldsymbol{x}_t', \boldsymbol{y}_t']'$, $\boldsymbol{h}_0 = [\boldsymbol{c}_x', \boldsymbol{c}']'$ and $\boldsymbol{\varepsilon}_t = [\boldsymbol{\eta}_{x,t}', \boldsymbol{\eta}_t']'$. In this structural specification, $\boldsymbol{H}_0$ captures the contemporaneous relations between the variables. Provided that $\boldsymbol{H}_0$ is invertible, i.e., the structural model Equation (A.17) is assumed to be stable, we obtain the reduced-form VAR given by

$$\boldsymbol{z}_t = \boldsymbol{k}_0 + \sum_{\ell=1}^{\max(p,q,q_x)} \boldsymbol{K}_\ell\boldsymbol{z}_{t-\ell} + \boldsymbol{u}_t, \tag{A.18}$$

where $\boldsymbol{k}_0 = \boldsymbol{H}_0^{-1}\boldsymbol{h}_0$, $\boldsymbol{K}_\ell = \boldsymbol{H}_0^{-1}\boldsymbol{H}_\ell$ for all lags, and the residuals $\boldsymbol{u}_t = \boldsymbol{H}_0^{-1}\boldsymbol{\varepsilon}_t$ with $\mathbb{E}[\boldsymbol{u}_t\boldsymbol{u}_t'] = \boldsymbol{H}_0^{-1}\boldsymbol{\Sigma}_e\big(\boldsymbol{H}_0^{-1}\big)' = \boldsymbol{\Sigma}_u$. Note that in light of the structural relation $\boldsymbol{u}_t = \boldsymbol{C}\boldsymbol{\varepsilon}_t$, it holds that $\boldsymbol{C} = \boldsymbol{H}_0^{-1}$.

Bayesian Estimation Procedure

In this section we discuss the Bayesian estimation method we use to obtain the parameters of the reduced-form VAR of the domestic models and common variable models, (23) and (25). Following Lütkepohl (2005), let the model below denote a general matrix notation for a VARX(p, q) models, with n endogenous variables and n_{ex} exogenous variables. That is,

$$\boldsymbol{Y} = \boldsymbol{X}\boldsymbol{B} + \boldsymbol{E}, \tag{A.19}$$

where $\boldsymbol{Y}$ is a $(T-p)\times n$ matrix containing the n endogenous variables. The right-hand side $(T-p)\times(np+n_{ex}(q+1)+1)$ matrix $\boldsymbol{X}$ containing all lags of the VAR, including exogenous variables, and a constant, and $\boldsymbol{B}$ denotes the corresponding coefficient matrix. The residuals $\boldsymbol{E}$ have variance-covariance matrix $\boldsymbol{\Sigma}$.

The prior on $\boldsymbol{B}$ and $\boldsymbol{\Sigma}$ is an independent normal-inverted Wishart prior, such that $p(\boldsymbol{B}, \boldsymbol{\Sigma}) = p(\boldsymbol{B})p(\boldsymbol{\Sigma})$, with

$$\boldsymbol{\Sigma} \sim \mathcal{IW}(\boldsymbol{S}_0, \upsilon_0) \propto |\boldsymbol{\Sigma}|^{-\upsilon_0/2} \exp\Big(-\frac{1}{2}\mathrm{tr}(\boldsymbol{S}_0)\boldsymbol{\Sigma}^{-1}\Big), \tag{A.20}$$

and

$$\text{vec}(\boldsymbol{B}) \sim \mathcal{N}(\text{vec}(\boldsymbol{B}_0), \boldsymbol{V}_0) \propto \exp\Big(-\frac{1}{2}\text{vec}(\boldsymbol{B}-\boldsymbol{B}_0)'\boldsymbol{V}_0^{-1}\text{vec}(\boldsymbol{B}-\boldsymbol{B}_0)\Big), \tag{A.21}$$

where vec is the vectorization operator, $\mathcal{IW}$ is the inverted-Wishart distribution and $\mathcal{N}$ is the normal distribution.

The prior parameter $v_0 = N + 2$ and S_0 is a diagonal matrix with σ_i^2 on its diagonal, where σ_i denotes the standard error in a $AR(p)$ model of variable i. In $\boldsymbol{B}_0$ we set the coefficient the diagonal element corresponding to the first lag to one if the corresponding variable is non-stationary according to the ADF test (Dickey and Fuller, 1979), and zero otherwise. All remaining entries are zero. The matrix $\boldsymbol{V}_0$ is a diagonal matrix, where each element corresponds to the implied standard deviation of lag ℓ of variable j in equation i, which is equal to $\lambda_1\sigma_i/\sigma_j\ell^{-\lambda_2}$. We set $\lambda_1 = 0.2, \lambda_2 = 1$ following Litterman (1986).

The posterior distribution of $\boldsymbol{\Sigma}$ is

$$\boldsymbol{\Sigma}|\boldsymbol{B}, \boldsymbol{X} \sim \mathcal{IW}(\overline{\boldsymbol{S}}, \overline{v}), \text{ with } \overline{\boldsymbol{S}} = \boldsymbol{S}_0 + \boldsymbol{E}'\boldsymbol{E} \text{ and } \overline{v} = v_0 + T, \tag{A.22}$$

where the latter two equations are updating equations. The posterior distribution of $\boldsymbol{B}$ is

$$\begin{aligned} \text{vec}(\boldsymbol{B})|\boldsymbol{\Sigma}, \boldsymbol{X} &\sim \mathcal{N}(\text{vec}(\overline{\boldsymbol{B}}), \overline{\boldsymbol{V}}), \\ \overline{\boldsymbol{V}} = \Big(\boldsymbol{V}_0^{-1} + \boldsymbol{\Sigma}^{-1} \otimes \boldsymbol{X}'\boldsymbol{X}\Big)^{-1}&, \text{ and } \text{vec}(\overline{\boldsymbol{B}}) = \overline{\boldsymbol{V}}\Big(\boldsymbol{V}_0^{-1}\text{vec}(\boldsymbol{B}_0) + (\boldsymbol{\Sigma}^{-1} \otimes \boldsymbol{X}')\text{vec}(\boldsymbol{Y})\Big). \end{aligned} \tag{A.23}$$

We use Gibbs sampling to compute the posterior distribution. To compute the complete posterior distribution, we sample in an iterative manner from (A.22) and (A.23) until the sampler converges.

GVAR Model Statistics

Below are model diagnostics reported. The left figure shows that there is indeed weak cross-sectional dependence in the idiosyncratic shocks—over 70% of the residuals have a contemporaneous correlation of lower than 0.2. The right figure shows that the majority of the residuals are weakly autocorrelated. The trade-based weights are indeed relatively small. We further assume that the trade-based weights and GDP weights are constant over time. This is a reasonable assumption, as the relative trade relations and relative GDPs between the four countries do not change too much in our sample. All in all, this GVAR specification seem to capture the complex dynamics between countries well, and adequately satisfy the GVAR assumptions.

Figure A.1: Model statistics GVAR

Pair correlation model residuals $\boldsymbol{u}_t$

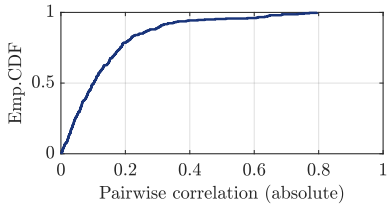

Autocorrelation residuals $\boldsymbol{\varepsilon}_t$

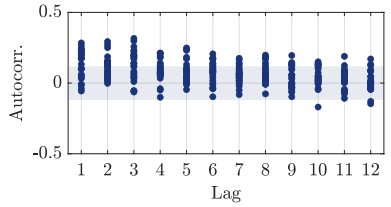

		Import				Eigenvalues	
		FRA	GER	ITA	SPN	Max.	Min.
Export	FRA	-	0.46	0.31	0.40	0.9965	0.0144
	GER	0.54	-	0.54	0.40		
	ITA	0.25	0.36	-	0.20		
	SPN	0.21	0.17	0.15	-		
	$\widetilde{\boldsymbol{w}}$ (GDP)	0.28	0.37	0.21	0.14		

Note: Autocorrelation and pairwise correlation is reported for the residuals in the two figures. The table reports the trade-based weights between the countries in 2014, the GDP weights between the countries, and the maximum and minimum eigenvalues of the median model.

Additional Results

Figure A.2: Impulse response functions to a monetary policy shock and simultaneous uncertainty shock in Italy and Spain, spill-overs and direct effects

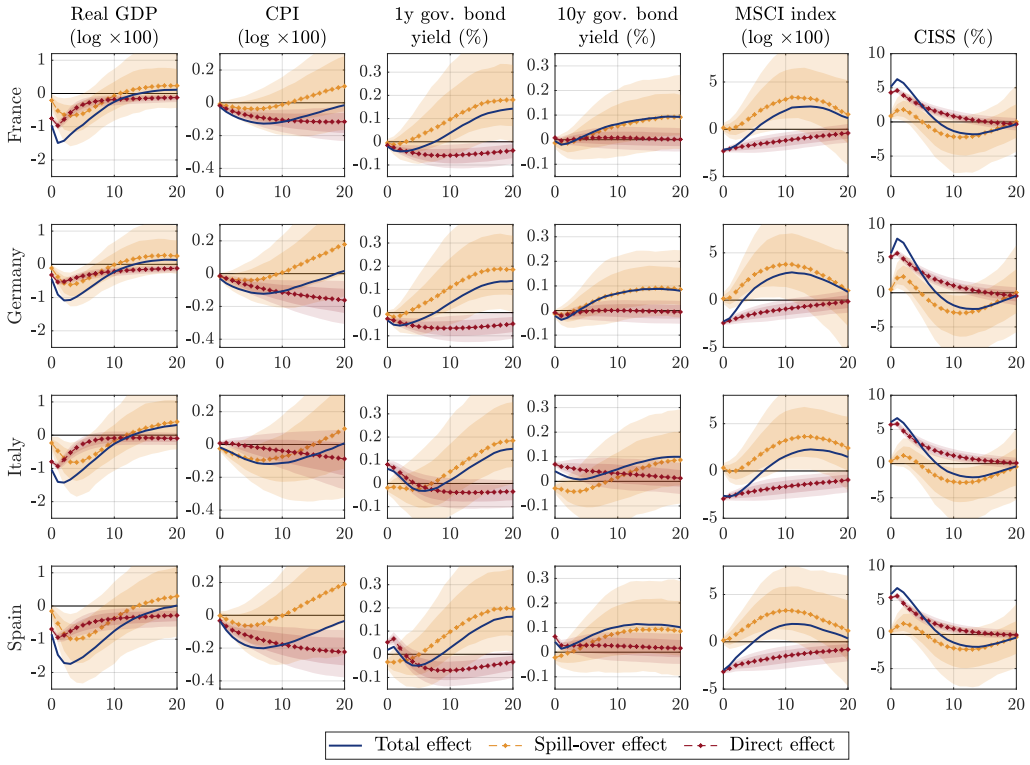

Note: All impulse responses correspond to the responses on a 20 month horizon. The solid dark blue lines correspond to the median multiple shock impulse response functions of a monetary policy shock combined with a shock in systematic risk in Italy and Spain. The darker (lighter) shaded areas correspond to 16–84th (5–95th) percentiles. The yellow lines correspond to the (coinciding) traditional and generalized median impulse responses to one monetary policy shock. The red and blue lines with correspond to the sum of the traditional and generalized median impulse response functions to all three shocks, respectively. The sample period is 01:1999-10:2022.

Figure A.3: Impulse response functions to a monetary policy shock and simultaneous uncertainty shock in Italy and Spain, 6 year horizon

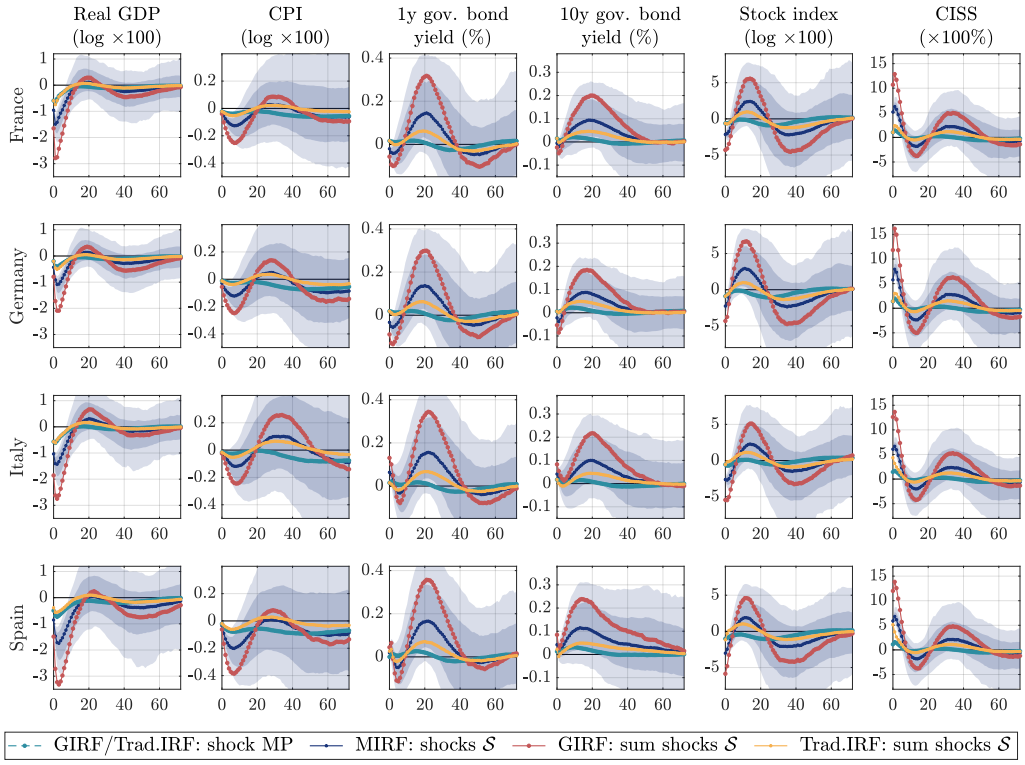

Note: All impulse responses correspond to the responses on a 6 year horizon. The solid dark blue lines correspond to the median multiple shock impulse response functions of a monetary policy shock combined with a shock in systematic risk in Italy and Spain. The darker (lighter) shaded areas correspond to 16–84th (5–95th) percentiles. The yellow lines correspond to the (coinciding) traditional and generalized median impulse responses to one monetary policy shock. The red and blue lines with correspond to the sum of the traditional and generalized median impulse response functions to all three shocks, respectively. The sample period is 01:1999-10:2022.

Figure A.4: Impulse response functions to a negative global equity shock, 6 year horizon

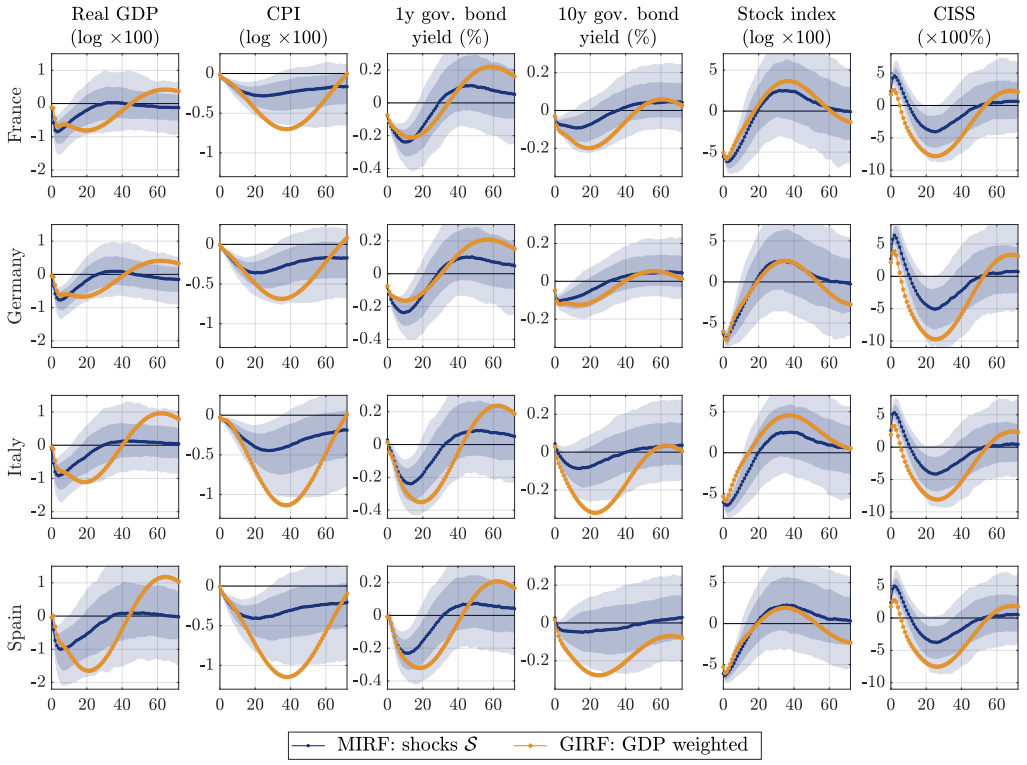

Note: All impulse responses correspond to the responses on a 6 year horizon. The solid dark blue lines correspond to the median multiple shock impulse response functions of an equity shock in all countries. The darker (lighter) shaded areas correspond to 16–84th (5–95th) percentiles. The orange lines correspond to generalized GDP-weighted median impulse responses to all four country-specific equity shocks. The sample period is 01:1999-10:2022.